Parameterization of Lakes in Numerical Weather Prediction. Part 1: Description of a Lake Model

Dmitrii V. Mironov[1†]

[1] German Weather Service, Offenbach am Main, Germany

December 17, 2005

Abstract

A lake model capable of predicting the surface temperature in lakes of various depth on the time scales from a few hours to a year is developed. The model is based on a two-layer parametric representation of the temperature profile, where the structure of the stratified layer between the upper mixed layer and the basin bottom, the lake thermocline, is described using the concept of self-similarity of the evolving temperature profile. The same concept is used to describe the temperature structure of the thermally active upper layer of bottom sediments and of the ice and snow cover. The model incorporates the heat budget equations for the four layers in question, viz., snow, ice, water and bottom sediments, developed with due regard for the vertically distributed character of the short-wave radiation heating. An entrainment equation is used to compute the depth of a convectively-mixed layer. A relaxation-type equation is used to compute the wind-mixed layer depth in stable and neutral stratification, where a multi-limit formulation for the equilibrium mixed-layer depth accounts for the effects of the earth's rotation, of the surface buoyancy flux and of the static stability in the thermocline. Simple thermodynamic arguments are invoked to develop the evolution equations for the ice and snow depths. The result is a computationally efficient bulk model that incorporates much of the essential physics.

Empirical constants and parameters of the proposed model are estimated, using independent empirical and numerical data. They should not be re-evaluated when the model is applied to a particular lake. The only lake-specific parameters are the lake depth, the optical characteristics of lake water, the temperature at the bottom of the thermally active layer of bottom sediments and the depth of this layer. In this way, the model does not require re-tuning, a procedure that may improve an agreement with a limited amount of data but should generally be avoided. The proposed lake model is intended for use in numerical weather prediction, climate modelling, and other numerical prediction systems for environmental applications. The present paper (Part 1) contains an overview of previous studies and the model description. In a companion paper (Part 2), the proposed model is tested against observational data through single-column numerical experiments.

1 Introduction

Lakes significantly affect the structure of the atmospheric surface layer and therefore the surface fluxes of heat, water vapour and momentum. This effect has not been systematically studied so far and is poorly understood. In most numerical weather prediction (NWP) systems, the effect of lakes is either entirely ignored or is parameterized very crudely. At present, a large number of small-to-medium size lakes are indistinguishable sub-grid scale

[†]Corresponding author address: Deutscher Wetterdienst, Abteilung Meteorologische Analyse und Modellierung, Referat FE14, Frankfurter Str. 135, D-63067 Offenbach am Main, Germany. Phone: +49-69-8062 2705, fax: +49-69-8062 3721. E-mail: Dmitrii.Mironov@dwd.de

features. These lakes will become resolved scale features as the horizontal resolution is increased. Then, a physically sound model is required to predict the lake surface temperature and the effect of lakes on the structure and transport properties of the atmospheric surface layer. Apart from being physically sound, a lake model must meet stringent requirements of computational economy.

The problem is twofold. For one thing, the interaction of the atmosphere with the underlying surface is strongly dependent on the surface temperature and its time-rate-of-change. It is common for NWP systems to assume that the water surface temperature can be kept "frozen" over the forecast period. That is, once the NWP model has been initialised, the surface temperature of the grid points of the type "water" is kept constant in time. The assumption is to some extent justified for seas and deep lakes. It is doubtful for small-to-medium size relatively shallow lakes, where the short-term variations of the surface temperature (with a period of several hours to one day) reach several degrees. A large number of such lakes will become resolved scale features as the horizontal resolution is increased. The use of a horizontal grid size of about three kilometres or even less will soon become a common practice in short-range weather forecast. In NWP systems with coarser resolution, many small-to-medium size lakes remain sub-grid scale features. However, the presence of these lakes cannot be ignored due to their aggregate effect on the grid-scale surface fluxes. This also holds for climate modelling systems concerned with the time scales ranging from many days to many years.

Another important aspect of the problem is that lakes strongly modify the structure and the transport properties of the atmospheric surface layer. A major outstanding question is the parameterization of the roughness of the water surface with respect to wind and to scalar quantities, such as potential temperature and specific humidity. This second aspect of the problem is beyond the scope of the present paper. It should be a subject for future studies.

A renewed interest in the problem of lakes has led to the development of several lake models for use in NWP and climate modelling systems (e.g. Ljungemyr et al. 1996, Goyette et al. 2000, Tsuang et al. 2001). Some models assume a complete mixing down to the lake bottom and characterise the entire water column by a single value of temperature. Although this assumption results in a bulk model that is very cheap computationally, it is an oversimplification from the physical point of view. As most lakes are stratified over a considerable part of the year, using a bulk model where the mixed layer is assumed to always reach the bottom, i.e. neglecting the lake thermocline, results in large errors in the surface temperature. Turbulence closure models, e.g. models based on the transport equation for the turbulence kinetic energy (Tsuang et al. 2001), would do the work of describing the lake thermocline better. However, closure models are expensive computationally. Their use to treat a large number of lakes can hardly be afforded. Thus, a lake model is required that is physically sound, but at the same time computationally efficient.

In the present paper, a lake model capable of predicting the surface temperature in lakes of various depth on the time scales from a few hours to a year is developed. The model is based on a two-layer parameterization of the temperature profile, where the structure of the stratified layer between the upper mixed layer and the basin bottom, the lake thermocline, is described using the concept of self-similarity of the evolving temperature profile. The same concept is used to describe the interaction of the water column with bottom sediments and the evolution of the ice and snow cover. This approach, that is based on what could be called "verifiable empiricism" but still incorporates much of the essential physics, offers a very good compromise between physical realism and computational economy. In section 2, the concept of self-similarity of the temperature profile is outlined and a brief overview

of previous studies along this line is given. A lake model is developed in section 3. In section 4, we draw conclusions from the present study. In a companion paper (Part 2), the proposed lake model is tested against observational data through single-column numerical experiments. Future work should include (i) developing and testing the atmospheric surface-layer parameterization scheme that accounts for specific features of the surface air layer over lakes, and (ii) integrating and testing the new lake model and the new surface-layer scheme in the full three-dimensional NWP system environment. Results will be described in subsequent papers.

2 Background

2.1 The Concept of Self-Similarity of the Temperature Profile

The concept of self-similarity of the temperature profile $\theta(z,t)$ in the thermocline was put forward by Kitaigorodskii and Miropolsky (1970) to describe the vertical temperature structure of the oceanic seasonal thermocline. The essence of the concept is that the dimensionless temperature profile in the thermocline can be fairly accurately parameterized through a "universal" function of dimensionless depth, that is

$$\frac{\theta_s(t)-\theta(z,t)}{\Delta\theta(t)}=\Phi_\theta(\zeta) \quad \text{at} \;\; h(t)\le z\le h(t)+\Delta h(t). \tag{1}$$

Here, t is time, z is depth, $\theta_s(t)$ is the temperature of the upper mixed layer of depth $h(t)$, $\Delta\theta(t)=\theta_s(t)-\theta_b(t)$ is the temperature difference across the thermocline of depth $\Delta h(t)$, $\theta_b(t)$ is the temperature at the bottom of the thermocline, and $\Phi_\theta\equiv[\theta_s(t)-\theta(z,t)]/\Delta\theta(t)$ is a dimensionless "universal" function of dimensionless depth $\zeta\equiv[z-h(t)]/\Delta h(t)$ that satisfies the boundary conditions $\Phi_\theta(0)=0$ and $\Phi_\theta(1)=1$. In what follows, the arguments of functions dependent on time and depth are not indicated, unless it is indispensable. The temperature profile given by Eq. (1) is illustrated in Fig. 1.

The idea of self-similarity of the temperature profile in the thermocline can be traced back to the famous work of Munk and Anderson (1948). Although these authors did not present Eq. (1) in its explicit form, the following quotation is a qualitative statement of the idea (Munk and Anderson 1948, p. 276):

> ...the upper layers are stirred until an almost homogeneous layer is formed, bounded beneath by a region of marked temperature gradient, the thermocline. ...If the wind increases in intensity the thermocline moves downward, but the characteristic *shape* of the temperature-depth curve remains essentially unchanged. (Original authors' italic.)

In this connection, the work of Ertel (1954) should be mentioned. Ertel considered the formation and deepening of the thermocline in a fresh-water lake during the summer heating period, using an analytical solution to the linear heat transfer equation. Following Birge, he defined the thermocline ("thermische Sprungschicht" – the temperature jump layer, as termed in op. cit.) as a layer where the vertical temperature gradient exceeds 1 $\mathrm{K\cdot m^{-1}}$. Ertel did not present his results in the form given by Eq. (1). He found, however, that the ratio of the depth from the upper boundary of the thermocline to the bend point of the temperature profile to the depth from the bend point to the bottom of the thermocline is constant. In other words, the *shape* of the temperature-depth curve in the thermocline is independent of time.

Notice that the concept of self-similarity of the temperature profile in the thermocline can be considered as a natural extension of the concept of the temperature uniform mixed layer that has been successfully used in geophysical fluid dynamics over several decades. Indeed, using the mixed-layer temperature θ_s and its depth h as appropriate scales, the mixed-layer concept can be expressed as $\theta(z,t)/\theta_s(t) = \vartheta[z/h(t)]$, where a dimensionless function ϑ is simply a constant equal to one. The use of $\Delta\theta$ and Δh as appropriate scales of temperature and depth, respectively, in the thermocline leads to Eq. (1), where Φ_θ is not merely a constant but a more sophisticated function of ζ. We emphasise that neither the mixed-layer concept nor the concept of self-similarity of the thermocline is well justified theoretically. Both concepts heavily rely on empirical evidence and should therefore be considered phenomenological. However, this phenomenological approach appears to describe the observed temperature structure to a degree of approximation that is sufficient for many applications.

2.2 Empirical Evidence

In order to obtain an analytical approximation of the dimensionless function $\Phi_\theta(\zeta)$ in Eq. (1), Kitaigorodskii and Miropolsky (1970) took a geometrical approach similar to what is often referred to as the Polhausen method in the boundary-layer theory. They expressed Φ_θ as a fourth-order polynomial in ζ and invoked five boundary conditions to specify the polynomial coefficients. Apart from the above two conditions $\Phi_\theta(0) = 0$ and $\Phi_\theta(1) = 1$ that simply follow from the definition of Φ_θ and ζ, they assumed neutral temperature stratification at the bottom of the thermocline, $\Phi'_\theta(1) = 0$, and a smooth matching to the temperature profile in the underlying layer, $\Phi''_\theta(1) = 0$. Furthermore, they assumed that the temperature-depth curve has a maximum curvature at the upper boundary of the thermocline, $\Phi'''_\theta(0) = 0$. The resulting expression,

$$\Phi_\theta = \frac{8}{3}\zeta - 2\zeta^2 + \frac{1}{3}\zeta^4, \tag{2}$$

was tested against monthly-mean temperature profiles recorded at the ocean weather ships "Papa" (Kitaigorodskii and Miropolsky 1970) and "Tango" (Kitaigorodskii 1970).

A reasonable polynomial approximation of $\Phi_\theta(\zeta)$ was proposed by Arsenyev and Felzenbaum (1977). These authors also took a geometrical approach (the Polhausen method) but, unlike Kitaigorodskii and Miropolsky (1970), did not make use of the condition $\Phi'''_\theta(0) = 0$. The resulting third-order polynomial,

$$\Phi_\theta = 1 - (1-\zeta)^3, \tag{3}$$

has subsequently enjoyed wide popularity.

The concept of self-similarity of the temperature profile in the thermocline received support through laboratory studies (Linden 1975, Voropaev 1977, Wyatt 1978). Linden (1975) modified the Kitaigorodskii and Miropolsky (1970) expression (2) in order to account for the stable density stratification in a quiescent layer below the thermocline. He proposed the expression (in op. cit., it is given in terms of density)

$$\Phi_\theta = \zeta + (1-\Gamma)\left(\frac{5}{3}\zeta - 2\zeta^2 + \frac{1}{3}\zeta^4\right), \tag{4}$$

where $\Gamma = -(\Delta\theta/\Delta h)^{-1}(\partial\theta/\partial z)|_{h+\Delta h}$ is the temperature gradient just below the thermocline relative to the mean temperature gradient within the thermocline [by virtue of a smooth matching of the temperature profile in the thermocline and in the layer below, $\Gamma = \Phi'_\theta(1)$]. Equation (4) revealed a good agreement with data from measurements in a laboratory tank, where turbulence was generated by an oscillating grid.

Empirical data taken in natural conditions (Miropolsky et al. 1970, Nesterov and Kalatsky 1975, Kharkov 1977, Reshetova and Chalikov 1977, Efimov and Tsarenko 1980, Filyushkin and Miropolsky 1981, Mälkki and Tamsalu 1985, Tamsalu and Myrberg 1998) also lent support to the concept of self-similarity of the thermocline. However, the scatter of data around the temperature-depth curves proved to be quite large. Reshetova and Chalikov (1977) attempted to extend the self-similarity concept to parameterize the vertical profile of salinity in the ocean.

Filyushkin and Miropolsky (1981) noticed that the shape of the temperature-depth curve depends on the mixed-layer state. They proposed to differentiate between the two cases: the mixed-layer deepening, $dh/dt > 0$, and its stationary state or retreat, $dh/dt \leq 0$. Mälkki and Tamsalu (1985) developed the following empirical approximations for these two cases:

$$\Phi_\theta = \begin{cases} 1-(1-\zeta)^3 & \text{if} \quad dh/dt > 0 \\ 1-4(1-\zeta)^3+3(1-\zeta)^4 & \text{if} \quad dh/dt \leq 0. \end{cases} \tag{5}$$

These expressions were tested against data from measurements in the Baltic Sea (Mälkki and Tamsalu 1985, Tamsalu and Myrberg 1998). The first line of Eq. (5) that corresponds to the mixed-layer deepening coincides with Eq. (3) developed from simple geometrical arguments by Arsenyev and Felzenbaum (1977). In case of the mixed-layer stationary state or retreat, the form of the temperature-depth curve is essentially different. The temperature profiles in the thermocline and in the mixed layer match smoothly, and the vertical temperature gradient is a maximum within the thermocline, not at its upper boundary. Data taken in Lake Ladoga, Russia, and Lake Sevan, Armenia, corroborated the occurrence of two types of self-similar temperature profiles in the thermocline (Zilitinkevich 1991).

2.3 Theoretical Explanation

A plausible theoretical explanation for the observed self-similarity of the temperature profile in the thermocline was offered in case of the mixed-layer deepening (Barenblatt 1978, Turner 1978, Shapiro 1980, Zilitinkevich et al. 1988, Zilitinkevich and Mironov 1989, Mironov 1990, Zilitinkevich and Mironov 1992). These authors analysed the heat transfer equation

$$\frac{\partial\theta}{\partial t} = \frac{\partial}{\partial z} K_H \frac{\partial\theta}{\partial z}, \tag{6}$$

where K_H is the temperature conductivity (the heat conductivity divided by the density ρ and specific heat c of the medium in question). Introducing a vertical co-ordinate moving with the mixed layer-thermocline interface, $z' = z - h(t)$, they considered a travelling wave-type solution to Eq. (6). Assuming constant temperatures at the upper and lower boundaries of the thermocline, $\partial\theta_s/\partial t = \partial\theta_b/\partial t = 0$, Eq. (6) becomes

$$-\dot{h}\frac{d\theta}{dz'} = \frac{d}{dz'} K_H \frac{d\theta}{dz'}, \tag{7}$$

where $\dot{h} \equiv dh/dt > 0$ is the rate of the mixed-layer deepening.

Barenblatt (1978) took K_H to be constant and considered a solution to Eq. (7) in a half-space $z' > 0$. Using boundary conditions $\theta = \theta_s$ at $z' = 0$ and $\theta = \theta_b$ at $z' = \infty$, the solution reads

$$\Phi_\theta = 1 - \exp(-\dot{h}z'/K_H). \tag{8}$$

Since the thermocline has an infinite thickness, the above solution cannot be recast in terms of $\Phi_\theta(\zeta)$. However, Eq. (8) appears to be a fairly close approximation to the empirical

polynomials proposed by Kitaigorodskii and Miropolsky (1970) and Arsenyev and Felzenbaum (1977) at certain values of $\dot{h}/K_H$.

Turner (1978) examined both the simplest case of $K_H = const$ and a more sophisticated case, where K_H is proportional to the vertical temperature gradient,

$$K_H = -\frac{\dot{h}l^2}{\Delta\theta}\frac{\partial\theta}{\partial z}, \tag{9}$$

l being a characteristic eddy length scale. Assuming $K_H \propto -\partial\theta/\partial z$, he added the factor $\dot{h}l^2/\Delta\theta$ to the r.h.s. of Eq. (9) "to be consistent dimensionally". In support of Eq. (9), Turner considered generation of turbulence by breaking internal gravity waves. He wrote (Turner 1978, p. 6): "It seems likely that the energy required to produce this addition mixing below the surface layer will be supplied by internal waves propagating into the gradient region, and then breaking. ... Clearly, the wave breaking and the density distribution must be intimately linked: for a given energy level breaking will occur preferentially in regions where the density gradient is high." Numerical experiments with a mixed-layer model (Kamenkovich and Kharkov 1975, Gill and Trefethen, unpublished manuscript referred to by Turner 1978) lend some support to this idea. They show an improved fit to ocean data if the effective temperature conductivity in the thermocline is taken proportional to the vertical temperature (density) gradient. Taking $l = const$ and using boundary conditions $\theta = \theta_s$ at $z = h$ and $\theta = \theta_b$ at $z = h + \Delta h$, and an additional condition $\partial\theta/\partial z = 0$ at $z = h + \Delta h$ that serves to determine l, the solution to Eqs. (7) and (9) is

$$\Phi_\theta = 1 - (1-\zeta)^2, \qquad l = \frac{1}{2}\Delta h. \tag{10}$$

Obviously, it is difficult to give preference to the above expression for $\Phi_\theta(\zeta)$ over the expressions developed by Kitaigorodskii and Miropolsky (1970) and Arsenyev and Felzenbaum (1977), or vice versa, on purely empirical ground by virtue of a large scatter of empirical data.

Zilitinkevich et al. (1988) pointed out that Eq. (9) is not consistent with the proposed wave breaking mechanism of mixing in the thermocline, although the mechanism per se is physically credible. The point is that Eq. (9) does not contain the buoyancy parameter $\beta = g\alpha_T$, where g is the acceleration due to gravity and α_T is the thermal expansion coefficient, which must obviously be taken into account. Indeed, there would be no internal gravity waves and no wave breaking mechanism of mixing were it not for the density changes associated with the temperature changes and not for the gravity that cause the buoyancy effects in a temperature-stratified fluid. Using β, $\partial\theta/\partial z$ and l as the governing parameters, Zilitinkevich et al. (1988) invoked dimensional arguments to obtain the following expression for the effective temperature conductivity in the thermocline:

$$K_H = l^2 N, \tag{11}$$

where $N = (-\beta\partial\theta/\partial z)^{1/2}$ is the buoyancy frequency (the constant of proportionality is incorporated into l). It is easy to verify that Eqs. (7) and (11) subject to the same boundary conditions as used by Turner (1978) have the following solution:

$$\Phi_\theta = 1 - (1-\zeta)^3, \qquad l = 3^{-3/4}(\beta\Delta\theta)^{-1/4}\Delta h^{3/4}\dot{h}^{1/2}. \tag{12}$$

The above expression for the temperature profile shape function $\Phi_\theta(\zeta)$ appears to coincide with the third-order polynomial (3) developed earlier from simple geometrical arguments by Arsenyev and Felzenbaum (1977) and on the basis of empirical data by Mälkki and Tamsalu (1985).

In the models of Turner (1978) and Zilitinkevich et al. (1988), the eddy length scale l was treated as a bulk quantity characteristic of the thermocline as a whole. Zilitinkevich and Mironov (1992, see also Zilitinkevich and Mironov 1989, and Mironov 1990) proposed to treat l as a depth-dependent quantity. To this end, they employed the transport equation for the turbulence kinetic energy (TKE) in its stationary form,

$$\frac{\partial e}{\partial t} = -\frac{\partial F}{\partial z} - \beta\mathcal{Q} - \epsilon = 0, \tag{13}$$

where e is the TKE per unit mass, F is the vertical TKE flux (the sum of the third-order velocity correlations and the pressure-velocity correlation), $\mathcal{Q}$ is the vertical turbulent temperature flux, and ϵ is the TKE dissipation rate. The temperature flux is also referred to as the kinematic heat flux, that is the heat flux divided by the density ρ and specific heat c. A calligraphic letter is used to avoid confusion with the heat flux $Q = \rho c\mathcal{Q}$. The following expression that is known to hold in strongly stable layers (see e.g. Zeman and Tennekes 1977, Brost and Wyngaard 1978, Otte and Wyngaard 2001) was used to relate the length scale to the TKE:

$$l = \frac{e^{1/2}}{N}. \tag{14}$$

The problem was closed through the use of a down-gradient approximation for the fluxes,

$$\mathcal{Q} = -K_H\frac{\partial\theta}{\partial z}, \qquad F = -K_E\frac{\partial e}{\partial z}, \tag{15}$$

and the Kolmogorov-Heisenberg hypothesis for the eddy exchange coefficients and the TKE dissipation rate,

$$\frac{K_H}{C_H} = \frac{K_E}{C_E} = le^{1/2}, \qquad \epsilon = C_\epsilon\frac{e^{3/2}}{l}, \tag{16}$$

where C_H, C_E and C_ϵ are dimensionless constants.

Considering the problem in a half-space $z' > 0$, the travelling wave-type solution to Eqs. (7), (13), (14), (15) and (16) subject to boundary conditions $\theta = \theta_s$, $e = e_h$ at $z' = 0$ and $\theta = \theta_b$, $e = 0$ at $z' = \infty$ is

$$\Phi_\theta = 1 - \exp(E_* - E_*/\eta), \qquad 6^{1/2}\exp(-E_*)\int_\eta^1 \eta'^2\exp(E_*/\eta')d\eta' = \xi. \tag{17}$$

Here, $\eta^2 = e_h^{-1}e$ and $\xi = C_e^{-1/2}e_h^{-1/2}N_hz'$ are the dimensionless TKE and the dimensionless vertical co-ordinate, respectively, $E_* = C_H^{-1}(6C_e)^{1/2}e_h^{-1/2}\dot{h}$ is the dimensionless rate of the mixed-layer deepening, e_h and N_h are the TKE and the buoyancy frequency, respectively, at the mixed layer-thermocline interface $z = h$, and $C_e = C_E(C_H + C_\epsilon)^{-1}$ is a dimensionless constant. The solution (17) describes a family of the temperature-depth curves where the shape of the curve depends upon E_*. At $E_* \geq 2$, the vertical temperature gradient is a maximum at the mixed layer-thermocline interface, $z = h$, whereas at $E_* < 2$, the temperature gradient is a maximum at $z > h$. The temperature profile given by Eq. (17) is quite similar to the third-order polynomial (3) at certain values of E_*.

An extension of the $K_H = const$ solution to Eq. (7) was developed by Shapiro (1980). He assumed that the mixed-layer temperature θ_s and the rate of the mixed-layer deepening $\dot{h}$ do not remain constant, as in the case considered by Barenblatt (1978) and Turner (1978), but experience small-amplitude fluctuations. Then, an additional term appears on the r.h.s. of Eq. (7), namely $\left\langle \dot{h}"\partial\theta_s"/\partial z \right\rangle$, where the angle brackets denote an ensemble mean and a

quotation mark denotes a fluctuation therefrom. An analysis of the resulting solution showed an increase of the temperature gradient just below the mixed layer-thermocline interface and an overall cooling of the thermocline as compared to the case of constant θ_s and $\dot{h}$ when the fluctuations of θ_s and of $\dot{h}$ are coherent.

The analytical travelling wave-type solutions considered above are conditioned by a constant rate of the mixed-layer deepening and constant temperatures at the upper and lower boundaries of the thermocline. If these quantities are not constant but vary slowly with time, the analytical solutions are not exact but approximate. If these quantities undergo fast changes, a travelling wave-type solution to the heat transfer equation can no longer serve as a theoretical explanation for the observed self-similarity of the temperature profile in the thermocline. It should be pointed out that all the above theoretical models apply to the case of the mixed-layer deepening. No theoretical explanation for the self-similarity of the temperature profile in case of the mixed-layer stationary state or retreat has been offered so far. The self-similarity at $dh/dt \leq 0$ is based on the empirical evidence only and should therefore be considered purely phenomenological.

2.4 Bottom Sediments

A distinctive feature of shallow lakes is a strong thermal interaction between the water body and the bottom sediments. A sizable portion of the heat received from the atmosphere during spring and summer can be accumulated in the thermally active upper layer of bottom sediments. This heat is then returned back to the water column during autumn and winter, leading to a hysteresis-like behaviour of the seasonal temperature cycle of the water column-bottom sediment system. A straightforward approach to describe the evolution of the thermal structure of bottom sediments is to use the equation of heat transfer with a priori knowledge of the thermal diffusivity of sediments (see e.g. Gu and Stefan 1990, Fang and Stefan 1996, 1998, and references therein). The major shortcoming of this approach is that the thermal diffusivity is strongly dependent on the composition of the sediments and on the amount of organic matter they contain and is, therefore, rarely well known.

Golosov and Kreiman (1992) proposed an alternative way of describing the vertical temperature structure of bottom sediments. Their approach is based on a two-layer self-similar parametric representation of the evolving temperature profile in the sediments that is conceptually similar to a parametric representation of the temperature profile in the thermocline. Observations suggest (a summary of observational studies is given in Ryanzhin 1997) that the temperature profile in the bottom sediments has the form of a travelling thermal wave. Typical temperature profiles in the lake bottom sediments are illustrated in Fig. 2. The wave starts at the water-sediment interface $z = D$ and propagates downward as the lake water and the bottom sediments are heated during spring and summer. When heating ceases and cooling sets in, a new wave starts at $z = D$. It propagates downward as the lake water and the sediments are cooled during autumn and winter, thus closing the annual cycle. The layer $D \leq z \leq L$, where seasonal temperature changes take place, is the thermally active layer of bottom sediments. Importantly, a characteristic *shape* of the temperature-depth curve remains approximately the same. Motivated by this empirical evidence, a two-layer parametric representation of the temperature profile in the bottom sediments was proposed by Golosov and Kreiman (1992) and further developed by Golosov et al. (1998). The expression of Golosov et al. (1998) reads

$$\theta(z,t) = \begin{cases} \theta_b(t) - [\theta_b(t) - \theta_H(t)]\,\Phi_{B1}(\zeta_{B1}) & \text{at} \quad D \leq z \leq H(t) \\ \theta_H(t) - [\theta_H(t) - \theta_L]\,\Phi_{B2}(\zeta_{B2}) & \text{at} \quad H(t) \leq z \leq L. \end{cases} \tag{18}$$

Here, θ_L is the (constant) temperature at the outer edge $z = L$ of the thermally active layer

of the sediments, θ_H is the temperature at the depth H where the vertical temperature gradient is zero, and $\Phi_{B1} \equiv (\theta_b - \theta)/(\theta_b - \theta_H)$ and $\Phi_{B2} \equiv (\theta_H - \theta)/(\theta_H - \theta_L)$ are dimensionless functions of dimensionless depths $\zeta_{B1} \equiv (z-D)/(H-D)$ and $\zeta_{B2} \equiv (z-H)/(L-H)$, respectively. Using empirical polynomial approximations of $\Phi_{B1}(\zeta_{B1})$ and $\Phi_{B2}(\zeta_{B2})$, Golosov et al. (1998) developed a simple procedure for calculating the heat flux through the water-sediment interface. Simulations of the seasonal cycle of temperature in the bottom sediments of several lakes using this procedure showed a satisfactory agreement with observations (Golosov et al. 1998, Kondratiev et al. 1998). In the present study, the approach of Golosov and Kreiman (1992) and Golosov et al. (1998) is used to develop a simple parameterization for calculating the heat flux through the water-sediment interface. It is presented in section 3.3.

A plausible theoretical explanation for the observed self-similarity of the temperature profile in bottom sediments was offered by Mironov et al. (2003). Assuming a travelling wave-type behaviour of the temperature profile, these authors considered the temperature distribution in the layer from the water-sediment interface $z = D$ to the depth $z = H$ penetrated by the wave. They showed that in the simplest case of constant temperature diffusivity K_H the heat transfer equation (6) subject to the boundary conditions $\Phi_{B1}(0) = 0$ and $\Phi_{B1}(1) = 1$ has an analytical solution in the form

$$\Phi_{B1} = \frac{\Pi_D}{\Pi_D - \Pi_H} \left(1 + \frac{\exp\left(-E\zeta_{B1}^2/4\right)}{\zeta_{B1}^{1/2}} \times \right.$$

$$\left. \left\{ P \left[\frac{W_{p,1/4}(E/2)}{M_{p,1/4}(E/2)} M_{p,1/4}(E\zeta_{B1}^2/2) - W_{p,1/4}(E\zeta_{B1}^2/2) \right] - \frac{\Pi_H}{\Pi_D} \exp(E/4) \right\} \right). \qquad (19)$$

Here, $E = K_H^{-1}(H-D)dH/dt$ is the dimensionless rate of propagation of the thermal wave, and $\Pi_D = K_H^{-1}(\theta_b - \theta_H)^{-1}(H-D)^2 d\theta_b/dt$ and $\Pi_H = K_H^{-1}(\theta_b - \theta_H)^{-1}(H-D)^2 d\theta_H/dt$ are the dimensionless time-rates-of-change of the temperature at the water-sediment interface $z = D$ and at the depth $z = H$ penetrated by the wave, respectively, $P = 2^{1/4}\pi^{-1/2}E^{-1/4}$ $\Gamma\left[(2E + \Pi_D - \Pi_H)/2E\right]$, $p = -\left[2(\Pi_D - \Pi_H) + E\right]/4E$, Γ is the Gamma function, and M and W are the Whittaker functions (Abramowitz and Stegun 1964, Chapter 13).

The solution (19) is conditioned by a constant dimensionless propagation rate of the thermal wave and constant time-rates-of-change of the temperature at the water-sediment interface and at the depth penetrated by the wave. In case E, Π_D and Π_H are not constant but vary slowly with time, Eq. (19) is not exact but approximate. If these quantities undergo fast changes, the analytical solution (19) can no longer serve as a theoretical explanation for the observed self-similarity of the temperature profile in bottom sediments. Equation (19) appears to compare favourably with data from measurements in a number of lakes, with data from laboratory experiments and with a phenomenological polynomial approximation of the temperature profile in bottom sediments developed by Golosov et al. (1998) on the basis of empirical data.

2.5 Ice and Snow Cover

Many lakes are frozen over a considerable part of the year so that the atmosphere does not directly communicate with the lake water. The atmosphere-lake interaction occurs through the air-ice or, if snow is present, through the air-snow interface. An ice-snow model is therefore required to predict the surface temperature. Use of sophisticated ice models with rheology is a standard practice in climate modelling where the integration is performed over many decades. The reader is referred to `http://stommel.tamu.edu/~baum/ocean_models.html`, where detailed descriptions of several dynamic-thermodynamic ice models and further references can

be found. For NWP and related applications, a sophisticated dynamic-thermodynamic ice model is not required (and most often cannot be afforded because of the high computation cost). A simplified thermodynamic model is usually sufficient. Such model is developed in section 3.4. As regards the thermodynamics of ice and snow, the model is broadly similar to most other models developed to date (summaries are given by Leppäranta 1993, and Launiainen and Cheng 1998). A distinguishing feature of the present model is the treatment of the heat transfer through the ice-snow cover. Most currently used ice models carry the heat transfer equation that is solved on a finite difference grid where the number of grid points and the grid spacing differ with the application. We use the integral, or bulk, approach. It is based on a parametric representation of the temperature profile within ice and snow and on the (integral) heat budgets of the ice and snow layers.

2.6 Applications

A number of computationally-efficient models based on the self-similar representation of the temperature profile have been developed and successfully applied to simulate the evolution of the mixed layer and seasonal thermocline in the ocean (Kitaigorodskii and Miropolsky 1970, Miropolsky 1970, Kitaigorodskii 1970, Kamenkovich and Kharkov 1975, Arsenyev and Felzenbaum 1977, and references therein, Kharkov 1977, Filyushkin and Miropolsky 1981). Filyushkin and Miropolsky (1981) assumed that both the temperature profile and the profile of the vertical heat flux in the thermocline can be represented in a self-similar form. We return to this issue in section 3.2.1. The self-similarity concept has also been applied to model the atmospheric convectively mixed layer capped by the temperature inversion (Deardorff 1979, Fedorovich and Mironov 1995, Mironov 1999, Pénelon et al. 2001).

Models of the seasonal cycle of temperature and mixing in medium-depth fresh-water lakes, based on the self-similar representation of the evolving temperature profile, have been developed and successfully applied by Zilitinkevich and Rumyantsev (1990), Zilitinkevich (1991), Mironov et al. (1991), Zilitinkevich et al. (1992), Mironov (1992), Golosov et al. (1998) and Kondratiev et al. (1998). A first attempt has been made to apply the above self-similarity concept to shallow lakes and to consider short-term (diurnal) variations of temperature and mixing conditions (Kirillin 2001a,b). This issue is addressed in the present study. As different from the ocean and the atmosphere, where the thermocline (capping inversion) is underlain (overlain) by a deep stably or neutrally stratified quiescent layer, the above lake models assume a two-layer temperature structure, where the thermocline extends from the bottom of the mixed layer down to the basin bottom. This assumption is fair for most lakes, except for very deep lakes such as Lake Baikal.

3 Model Description

In this section, we develop a lake model based on a self-similar parametric representation (assumed shape) of the evolving temperature profile in the water column, in the bottom sediments and in the ice and snow. The same basic concept is used to describe the temperature structure of the four media in question (snow, ice, water and sediment). The lake model proposed by Mironov et al. (1991) is taken as a starting point. It is modified and further developed to account for specific features of shallow lakes and to consider both long-term (seasonal) and short-term (diurnal) variations of temperature and mixing conditions. The lake water is treated as a Boussinesq fluid, i.e. the water density is taken to be constant equal to the reference density except when it enters the buoyancy term in the TKE equation and the expression for the buoyancy frequency. The other thermodynamic parameters are

considered constant except for the snow density and the snow heat conductivity (see section 3.5.3 and Appendix B).

The model presented in what follows is a bulk model. It incorporates the heat budget equations for the layers in question. An entrainment equation for the depth of a convectively-mixed layer and a relaxation-type equation for the depth of a wind-mixed layer in stable and neutral stratification are developed on the basis of the TKE equation integrated over the mixed layer. Simple thermodynamic arguments are invoked to develop the evolution equations for the ice and snow depths. The resulting system of ordinary differential equations for the time-dependent prognostic quantities that characterise the evolving temperature profile, see Fig. 3, is closed with algebraic (or transcendental) equations for diagnostic quantities, such as the heat flux through the lake bottom or the equilibrium wind-mixed layer depth. Finally, we end up with a lake model that is very cheap computationally but still incorporates much of the essential physics.

3.1 Equation of State

We utilise the quadratic equation of state of the fresh water,

$$\rho_w = \rho_r \left[1 - \frac{1}{2} a_T \left(\theta - \theta_r\right)^2\right], \tag{20}$$

where ρ_w is the water density, $\rho_r = 999.98 \approx 1.0 \cdot 10^3$ kg·m^{-3} is the maximum density of the fresh water at the temperature $\theta_r = 277.13$ K, and $a_T = 1.6509 \cdot 10^{-5}$ K^{-2} is an empirical coefficient (Farmer and Carmack 1981). Equation (20) is the simplest equation of state that accounts for the fact that the temperature of maximum density of the fresh water exceeds its freezing point $\theta_f = 273.15$ K. According to Eq. (20), the thermal expansion coefficient α_T and the buoyancy parameter β depend on the water temperature,

$$\beta(\theta) = g\alpha_T(\theta) = g a_T(\theta - \theta_r), \tag{21}$$

where $g = 9.81$ m·s^{-2} is the acceleration due to gravity.

3.2 The Water Temperature

3.2.1 Parameterization of the Temperature Profile and the Heat Budget

We adopt the following two-layer parameterization of the vertical temperature profile:

$$\theta = \begin{cases} \theta_s & \text{at} \quad 0 \le z \le h \\ \theta_s - (\theta_s - \theta_b)\Phi_\theta(\zeta) & \text{at} \quad h \le z \le D, \end{cases} \tag{22}$$

where $\Phi_\theta \equiv (\theta_s - \theta) / (\theta_s - \theta_b)$ is a dimensionless function of dimensionless depth $\zeta \equiv (z - h) / (D - h)$. The thermocline extends from the mixed-layer outer edge $z = h$ to the basin bottom $z = D$.

According to Eq. (22), h, D, θ_s, θ_b and the mean temperature of the water column, $\overline{\theta} \equiv D^{-1} \int_0^D \theta dz$, are related through

$$\overline{\theta} = \theta_s - C_\theta(1 - h/D)(\theta_s - \theta_b), \tag{23}$$

where

$$C_\theta = \int_0^1 \Phi_\theta(\zeta) d\zeta \tag{24}$$

is the shape factor.

The parameterization of the temperature profile (22) should satisfy the heat transfer equation

$$\frac{\partial}{\partial t}(\rho c\theta) = -\frac{\partial}{\partial z}(Q + I), \tag{25}$$

where Q is the vertical turbulent heat flux, and I is the heat flux due to short-wave radiation.

Integrating Eq. (25) over z from 0 to D yields the equation of the total heat budget,

$$D\frac{d\overline{\theta}}{dt} = \frac{1}{\rho_w c_w}\left[Q_s + I_s - Q_b - I(D)\right], \tag{26}$$

where c_w is the specific heat of water, Q_s and I_s are the values of Q and I, respectively, at the lake surface, and Q_b is the heat flux through the lake bottom. The radiation heat flux I_s that penetrates into the water is the surface value of the incident short-wave radiation flux from the atmosphere multiplied by $1 - \alpha_w$, α_w being the albedo of the water surface with respect to the short-wave radiation. The surface flux Q_s is a sum of the sensible and latent heat fluxes and the net heat flux due to long-wave radiation at the air-water interface. It is a rather sophisticated function of the surface air layer parameters, of cloudiness and of the surface temperature.

Integrating Eq. (25) over z from 0 to h yields the equation of the temperature budget in the mixed layer,

$$h\frac{d\theta_s}{dt} = \frac{1}{\rho_w c_w}\left[Q_s + I_s - Q_h - I(h)\right], \tag{27}$$

where Q_h is the heat flux at the bottom of the mixed layer.

Given the surface fluxes Q_s and I_s (these are delivered by the driving atmospheric model or are known from observations), and the decay law for the flux of short-wave radiation (section 3.5.3), Eqs. (23), (26) and (27) contain seven unknowns, namely, h, $\overline{\theta}$, θ_s, θ_b, Q_h, Q_b and C_θ. The mixed layer depth, the bottom heat flux and the shape factor are considered in section 3.2.2, section 3.3 and section 3.5.1, respectively. One more relation is required. Following Filyushkin and Miropolsky (1981, see also Tamsalu et al. 1997, and Tamsalu and Myrberg 1998), we assume that in case of the mixed layer deepening, $dh/dt > 0$, the profile of the vertical turbulent heat flux in the thermocline can be represented in a self-similar form. That is

$$Q = Q_h - (Q_h - Q_b)\Phi_Q(\zeta) \qquad \text{at } \; h \le z \le D, \tag{28}$$

where the shape function Φ_Q satisfies the boundary conditions $\Phi_Q(0) = 0$ and $\Phi_Q(1) = 1$. Equation (28) is suggested by the travelling wave-type solution to the heat transfer equation. If the mixed layer and the thermocline develop on the background of a deep stably or neutrally stratified quiescent layer (this situation is encountered in the ocean and in the atmosphere), the travelling wave-type solution shows that both the temperature profile and the profile of the turbulent heat flux are described by the same shape function, i.e. $\Phi_\theta(\zeta) = \Phi_Q(\zeta)$. In lakes, the thermocline usually extends from the bottom of the mixed layer down to the basin bottom. In this case, the travelling wave-type solution to the heat transfer equation also suggests self-similar profiles of the temperature and of the heat flux, however the relation between the shape functions $\Phi_\theta(\zeta)$ and $\Phi_Q(\zeta)$ is different. The issue is considered in Appendix A.

Integrating Eq. (25) with due regard for Eqs. (22) and (28) over z' from h to $z > h$, then integrating the resulting expression over z from h to D, we obtain

$$\frac{1}{2}(D-h)^2\frac{d\theta_s}{dt} - \frac{d}{dt}\left[C_{\theta\theta}(D-h)^2(\theta_s - \theta_b)\right] =$$

$$\frac{1}{\rho_w c_w}\left[C_Q(D-h)(Q_h-Q_b)+(D-h)I(h)-\int_h^D I(z)dz\right], \tag{29}$$

where

$$C_Q=\int_0^1 \Phi_Q(\zeta)d\zeta \tag{30}$$

is the shape factor with respect to the heat flux, and

$$C_{\theta\theta}=\int_0^1 d\zeta\int_0^{\zeta'}\Phi_\theta(\zeta')d\zeta' \tag{31}$$

is the dimensionless parameter. The analysis in Appendix A suggests that $C_Q=2C_{\theta\theta}/C_\theta$.

In case of the mixed-layer stationary state or retreat, $dh/dt\le 0$, Eq. (28) is not justified. Then, the bottom temperature is assumed to be "frozen",

$$\frac{d\theta_b}{dt}=0. \tag{32}$$

If $h=D$, then $\theta_b=\theta_s=\overline{\theta}$ and the mean temperature is computed from Eq. (26).

3.2.2 The Mixed-Layer Depth

Convection
Convective deepening of the mixed layer is described by the entrainment equation. This equation is conveniently formulated in terms of the dependence of the so-called entrainment ratio A on one or the other stratification parameter. The entrainment ratio is a measure of the entrainment efficiency. It is commonly defined as a negative of the ratio of the heat flux due to entrainment at the bottom of the mixed layer, Q_h, to an appropriate heat flux scale, Q_*. In case of convection driven by the surface flux, where the forcing is confined to the boundary, the surface heat flux Q_s serves as an appropriate flux scale. This leads to the now classical Deardorff (1970a, 1970b) convective scaling, where h and $|h\beta Q_s/(\rho_w c_w)|^{1/3}$ serve as the scales of length and velocity, respectively.

The Deardorff scaling is unsuitable for convective flows affected by the short-wave radiation heating that is not confined to the boundary but is distributed over the water column. If the mixed-layer temperature exceeds the temperature of maximum density, convective motions are driven by surface cooling, whereas radiation heating tends to stabilise the water column, arresting the mixed layer deepening (Soloviev 1979, Mironov and Karlin 1989). Such regime of convection is encountered in the oceanic upper layer (e.g. Kraus and Rooth 1961, Soloviev and Vershinskii 1982, Price et al. 1986) and in fresh-water lakes (e.g. Imberger 1985). If the mixed-layer temperature is below that of maximum density, volumetric radiation heating leads to de-stabilisation of the water column and thereby drives convective motions. Such regime of convection is encountered in fresh-water lakes in spring. Convective mixing often occurs under the ice, when the snow cover overlying the ice vanishes and solar radiation penetrates down through the ice (e.g. Farmer 1975, Mironov and Terzhevik 2000, Mironov et al. 2002, Jonas et al. 2003).

In order to account for the vertically distributed character of the radiation heating, we make use of a generalised convective heat flux scale

$$Q_*=Q_s+I_s+I(h)-2h^{-1}\int_0^h I(z)dz, \tag{33}$$

and define the convective velocity scale and the entrainment ratio as

$$w_* = [-h\beta(\theta_s)Q_*/(\rho_w c_w)]^{1/3}, \qquad A = -Q_h/Q_*, \tag{34}$$

respectively. In order to specify A, we employ the entrainment equation in the form

$$A + \frac{C_{c2}}{w_*}\frac{dh}{dt} = C_{c1}, \tag{35}$$

where C_{c1} and C_{c2} are dimensionless constants (the estimates of these and other empirical constants of our model are discussed in section 3.5.2 and summarised in Appendix B). The second term on the l.h.s. of Eq. (35) is the spin-up correction term introduced by Zilitinkevich (1975). This term prevents an unduly fast growth of h when the mixed-layer is shallow. If the spin-up term is small, Eq. (35) reduces to a simple relation $A = C_{c1}$ that proved to be a sufficiently accurate approximation for a large variety of geophysical and laboratory convective flows (Zilitinkevich 1991).

Equations (33), (34) and (35) should be used to compute the mixed-layer depth when the buoyancy flux $B_* = \beta(\theta_s)Q_*/(\rho_w c_w)$ is negative. The quantity $-hB_* \equiv w_*^3$ is a measure of the generation rate of the turbulence kinetic energy in a layer of depth h by the buoyancy forces (see a discussion in Mironov et al. 2002). A negative B_* indicates that the TKE is generated through convective instability. Otherwise, the TKE is lost to work against the gravity. This occurs when the density stratification is stable. A different formulation for the mixed-layer depth is then required.

Stable and Neutral Stratification

Mironov et al. (1991) used a diagnostic equation to determine the wind-mixed layer depth in stable and neutral stratification. That is, h was assumed to adjust to external forcing on a time scale that does not exceed the model time step. This assumption is fair if seasonal changes of temperature and mixing conditions are considered and the model time step is typically one day. The assumption is likely to be too crude to consider diurnal variations. To this end, we utilise a relaxation-type rate equation for the depth of a stably or neutrally stratified wind-mixed layer. It reads

$$\frac{dh}{dt} = \frac{h_e - h}{t_{rh}}. \tag{36}$$

Here, h_e is the equilibrium mixed-layer depth, and t_{rh} is the relaxation time scale given by

$$t_{rh} = \frac{h_e}{C_{rh}u_*}, \tag{37}$$

where $u_* = |\tau_s/\rho_w c_w|^{1/2}$ is the surface friction velocity, τ_s being the surface stress, and C_{rh} is a dimensionless constant. A rate equation (36) with the relaxation time scale proportional to the reciprocal of the Coriolis parameter was favourably tested by Zilitinkevich et al. (2002a) and Zilitinkevich and Baklanov (2002) against data from atmospheric measurements and was recommended for practical use.

In order to specify h_e, we make use of a multi-limit formulation for the equilibrium depth of a stably or neutrally stratified boundary layer proposed by Zilitinkevich and Mironov (1996). Based on the analysis of the TKE budget, these authors proposed a generalised equation for the equilibrium boundary-layer depth that accounts for the combined effects of rotation, surface buoyancy flux and static stability at the boundary-layer outer edge [Eq. (30) in op. cit.]. That equation reduces to the equations proposed earlier by Rossby and Montgomery (1935), Kitaigorodskii (1960) and Kitaigorodskii and Joffre (1988) in the limiting

cases of a truly neutral rotating boundary layer, the surface-flux-dominated boundary layer, and the imposed-stability-dominated boundary layer, respectively. It also incorporates the Zilitinkevich (1972) and the Pollard, Rhines and Thompson (1973) equations that describe the intermediate regimes, where the effects of rotations and stratification essentially interfere and are roughly equally important. We adopt a simplified version of the Zilitinkevich and Mironov (1996) equation [Eq. (26) in op. cit.] that does not incorporate the Zilitinkevich (1972) and the Pollard et al. (1973) scales. It reads

$$\left(\frac{fh_e}{C_n u_*}\right)^2 + \frac{h_e}{C_s L} + \frac{Nh_e}{C_i u_*} = 1, \tag{38}$$

where $f = 2\Omega \sin\phi$ is the Coriolis parameter, $\Omega = 7.29 \cdot 10^{-5}$ s^{-1} is the angular velocity of the earth's rotation, ϕ is the geographical latitude, L is the Obukhov length, N is the buoyancy frequency below the mixed layer, and C_n, C_s and C_i are dimensionless constants. We use a generalised formulation for the Obukhov length, $L = u_*^3/(\beta Q_*/\rho_w c_w)$, that accounts for the vertically distributed character of the radiation heating (note that we do not include the von Kármán constant in the definition of L). A mean-square buoyancy frequency in the thermocline, $\overline{N} = \left[(D-h)^{-1}\int_h^D N^2 dz\right]^{1/2}$, is used as an estimate of N in Eq. (38).

One further comment is in order. Zilitinkevich et al. (2002a) reconsidered the problem of the equilibrium stable boundary-layer depth. They concluded that the Zilitinkevich (1972) scale, $|u_* L/f|^{1/2}$, and the Pollard et al. (1973) scale, $u_*/|Nf|^{1/2}$, are the appropriate depth scales for the boundary layers dominated by the surface buoyancy flux and by the static stability at their outer edge, respectively. In other words, h_e depends on the Coriolis parameter no matter how strong the static stability. This is different from Eq. (38) where the limiting scales are L and u_*/N, respectively. The problem was examined further by Mironov and Fedorovich (2005). They showed that the above scales are particular cases of more general power-law formulations, namely, $h/L \propto (|f|L/u_*)^{-p}$ and $hN/u_* \propto (|f|/N)^{-p}$ for the boundary layers dominated by the surface buoyancy flux and by the static stability at their outer edge, respectively. The Zilitinkevich (1972) and Pollard et al. (1973) scales are recovered with $p = 1/2$, whereas the Kitaigorodskii (1960) and Kitaigorodskii and Joffre (1988) are recovered with $p = 0$. Scaling arguments are not sufficient to fix the exponent p. It should be evaluated on the basis of experimental data. Available data from observations and from large-eddy simulations are uncertain. They do not make it possible to evaluate p to sufficient accuracy and to conclusively decide between the alternative formulations for the boundary layer depth. Leaving this for future studies, we utilise Eq. (38). This simple interpolation formula is expected to be a sufficiently accurate approximation for most practical purposes (Mironov and Fedorovich 2005).

One more limitation on the equilibrium mixed-layer depth should be taken into account. Consider the situation where the mixed-layer temperature exceeds the temperature of maximum density, the surface flux Q_s is negative, whereas the heat flux scale Q_* given by Eq. (33) is positive (this can take place if $-Q_s/I_s < 1$). A positive Q_* indicates the the mixed layer of depth h is statically stable. A negative Q_s, however, indicates that convective instability should take place, leading to the development of a convectively mixed layer whose deepening is arrested by the radiation heating. The equilibrium depth h_c of such mixed layer is given by (see e.g. Mironov and Karlin 1989)

$$Q_*(h_c) = Q_s + I_s + I(h_c) - 2h_c^{-1}\int_0^{h_c} I(z)dz = 0. \tag{39}$$

This regime of convection is encountered on calm sunny days. If the wind suddenly ceases, Eq. (38) predicts a very shallow stably-stratified equilibrium mixed layer to which the mixed

layer of depth $h > h_e$ should relax. In fact, however, the mixed layer would relax towards a convectively mixed layer whose equilibrium depth is given by Eq. (39). In order to account for this constraint, we require that $h_e \geq h_c$ if $Q_*(h) > 0$ and $\theta_s > \theta_r$.

3.3 The Water - Bottom Sediment Interaction

3.3.1 Parameterization of the Temperature Profile and the Heat Budget

We adopt a two-layer parametric representation, Eq. (18), of the evolving temperature profile in the thermally active layer of bottom sediments proposed by Golosov et al. (1998). The parameterization (18) should satisfy the heat transfer equation (25), where the heat flux Q is due to molecular heat conduction and the bottom sediments are opaque to radiation. Integrating Eq. (25) over z from $z = D$ to $z = H$ with due regard for Eq. (18), we obtain

$$\frac{d}{dt}\left[(H-D)\theta_b - C_{B1}(H-D)(\theta_b - \theta_H)\right] - \theta_H \frac{dH}{dt} = \frac{1}{\rho_w c_w}\left[Q_b + I(D)\right], \tag{40}$$

where the heat flux at $z = H$ is zero by virtue of the zero temperature gradient there.

Integrating Eq. (25) over z from $z = H$ to $z = L$, we obtain

$$\frac{d}{dt}\left[(L-H)\theta_H - C_{B2}(L-H)(\theta_H - \theta_L)\right] + \theta_H \frac{dH}{dt} = 0, \tag{41}$$

where the heat flux at $z = L$, the geothermal heat flux, is neglected.

The shape factors C_{B1} and C_{B2} are given by

$$C_{B1} = \int_0^1 \Phi_{B1}(\zeta_{B1}) d\zeta_{B1}, \qquad C_{B2} = \int_0^1 \Phi_{B2}(\zeta_{B2}) d\zeta_{B2}. \tag{42}$$

3.3.2 Heat Flux through the Bottom

The bottom heat flux Q_b is due to molecular heat conduction through the uppermost layer of bottom sediments and can be estimated as the product of the negative of the temperature gradient at $z = D + 0$ and the molecular heat conductivity. The uppermost layer of bottom sediments is saturated with water. Its water content typically exceeds 90% and its physical properties, including the heat conductivity, are very close to the properties of the lake water. Then, the heat flux through the lake bottom is given by

$$Q_b = -\kappa_w \frac{\theta_H - \theta_b}{H - D} \Phi'_{B1}(0). \tag{43}$$

This relation closes the problem.

It should be stressed that Eqs. (40), (41) and (43) do not contain the molecular heat conductivity of bottom sediments, a quantity that is rarely known to a satisfactory degree of precision. It is through the use of the integral (bulk) approach, based on the parameterization (18) of the temperature profile, that the molecular heat conductivity of bottom sediments is no longer needed.

3.4 Ice and Snow Cover

In this section, we describe a two-layer thermodynamic (no rheology) model of the ice and snow cover. It is based on a self-similar parametric representation of the temperature profile within ice and snow and on the (integral) heat budgets of the ice and snow layers.

The approach is, therefore, conceptually similar to the approach used above to describe the temperature structure of the lake thermocline and of the thermally active layer of bottom sediments. Notice that the assumption about the shape of the temperature profile within the ice, the simplest of which is the linear profile, is either explicit or implicit in many ice models developed to date. A model of ice growth based on a linear temperature distribution was proposed by Stefan as early as 1891.

3.4.1 Parameterization of the Temperature Profile and the Heat Budget

We adopt the following parametric representation of the evolving temperature profile within ice and snow:

$$\theta(z,t) = \begin{cases} \theta_f - [\theta_f - \theta_I(t)]\Phi_I(\zeta_I) & \text{at} \quad -H_I(t) \le z \le 0 \\ \theta_I(t) - [\theta_I(t) - \theta_S(t)]\Phi_S(\zeta_S) & \text{at} \quad -[H_I(t) + H_S(t)] \le z \le -H_I(t). \end{cases} \tag{44}$$

Here, z is the vertical co-ordinate (positive downward) with the origin at the ice-water interface, H_I is the ice thickness, H_S is the thickness of snow overlaying the ice, θ_f is the fresh-water freezing point, θ_I is the temperature at the snow-ice interface, and θ_S is the temperature at the air-snow interface. Notice that the freezing point of salt water is a decreasing function of salinity. An extension of the present model that accounts for this dependence and is applicable to the ice over salt lakes or seas is presented by Mironov and Ritter (2004). Dimensionless universal functions $\Phi_I \equiv (\theta_f - \theta)/(\theta_f - \theta_I)$ and $\Phi_S \equiv (\theta_I - \theta)/(\theta_I - \theta_S)$ of dimensionless depths $\zeta_I \equiv -z/H_I$ and $\zeta_S \equiv -(z+H_I)/H_S$, respectively, satisfy the boundary conditions $\Phi_I(0) = 0$, $\Phi_I(1) = 1$, $\Phi_S(0) = 0$ and $\Phi_S(1) = 1$.

According to Eq. (44), the heat fluxes through the ice, Q_I, and through the snow, Q_S, due to molecular heat conduction are given by

$$Q_I = -\kappa_i \frac{\theta_f - \theta_I}{H_I} \frac{d\Phi_I}{d\zeta_I}, \qquad Q_S = -\kappa_s \frac{\theta_I - \theta_S}{H_S} \frac{d\Phi_S}{d\zeta_S}, \tag{45}$$

where κ_i and κ_s are the heat conductivities of ice and snow, respectively.

The parameterization of the temperature profile (44) should satisfy the heat transfer equation (25). Integrating Eq. (25) over z from the air-snow interface $z = -(H_I + H_S)$ to just above the ice-water interface $z = -0$ with due regard for the parameterization (44), we obtain the equation of the heat budget of the snow-ice cover,

$$\frac{d}{dt}\{\rho_i c_i H_I [\theta_f - C_I(\theta_f - \theta_I)] + \rho_s c_s H_S [\theta_I - C_S(\theta_I - \theta_S)]\} - \rho_s c_s \theta_S \frac{d}{dt}(H_I + H_S) =$$

$$Q_s + I_s - I(0) + \kappa_i \frac{\theta_f - \theta_I}{H_I} \Phi_I'(0). \tag{46}$$

Here, ρ_i and ρ_s are the densities of ice and of snow, respectively, c_i and c_s are specific heats of these media, and Q_s and I_s are the values of Q and I, respectively, at the air-snow or, if snow is absent, at the air-ice interface. The radiation heat flux I_s that penetrates into the interior of snow-ice cover is the surface value of the incident short-wave radiation flux from the atmosphere multiplied by $1 - \alpha_i$, α_i being the albedo of the ice or snow surface with respect to short-wave radiation. The dimensionless parameters C_I and C_S, the shape factors, are given by

$$C_I = \int_0^1 \Phi_I(\zeta_I) d\zeta_I, \qquad C_S = \int_0^1 \Phi_S(\zeta_S) d\zeta_S. \tag{47}$$

The heat flux at the snow-ice interface is assumed to be continuous, that is

$$-\kappa_i \frac{\theta_f - \theta_I}{H_I} \Phi_I'(1) = -\kappa_s \frac{\theta_I - \theta_S}{H_S} \Phi_S'(0). \tag{48}$$

Equations (46) and (48) serve to determine temperatures at the air-snow and at the snow-ice interfaces, when these temperatures are below the freezing point, i.e. when no melting at the snow surface (ice surface, when snow is absent) takes place. During the snow (ice) melting from above, the temperatures θ_S and θ_I remain equal to the freezing point θ_f, and the heat fluxes Q_S and Q_I are zero.

3.4.2 Snow and Ice Thickness

The equations governing the evolution of the snow thickness and of the ice thickness are derived from the heat transfer equation (25) that incorporates an additional term on its right-hand side, namely, the term $f_M(z) L_f dM/dt$ that describes the rate of heat release/consumption due to accretion/melting of snow and ice. Here, M is the mass of snow or ice per unit area, L_f is the latent heat of fusion, and $f_M(z)$ is a function that satisfies the normalization conditions $\int_{H_I}^{H_I+H_S} f_M(z)dz = 1$ and $\int_0^{H_I} f_M(z)dz = 1$ for snow and ice, respectively.

The accumulation of snow is not computed within the ice-snow model. The rate of snow accumulation is assumed to be a known time-dependent quantity that is provided by the atmospheric model or is known from observations. Then, the evolution of the snow thickness during the snow accumulation and no melting is computed from

$$\frac{d\rho_s H_S}{dt} = \left(\frac{dM_S}{dt}\right)_a, \tag{49}$$

where $M_S = \rho_s H_S$ is the snow mass per unit area, and $(dM_S/dt)_a$ is the (given) rate of snow accumulation.

When the temperature θ_I at the upper surface of the ice is below the freezing point θ_f, the heat conduction through the ice causes the ice growth. This growth is accompanied by a release of heat at the lower surface of the ice that occurs at a rate $L_f dM_I/dt$, where $M_I = \rho_i H_I$ is the ice mass per unit area. The normalization function f_M is equal to zero throughout the snow-ice cover except at the ice-water interface where $f_M = \delta(0)$, $\delta(z)$ being the Dirac delta function. Integrating Eq. (25) from $z = -0$ to $z = +0$ with due regard for this heat release yields the equation for the ice thickness. It reads

$$L_f \frac{d\rho_i H_I}{dt} = Q_w + \kappa_i \frac{\theta_f - \theta_I}{H_I} \Phi_I'(0), \tag{50}$$

where Q_w is the heat flux in the near-surface water layer just beneath the ice. If the r.h.s. of Eq. (50) is negative, i.e. the negative of the heat flux in the water, Q_w, exceeds the negative of the heat flux in the ice, $Q_I|_{z=0}$, ice ablation takes place.

As the atmosphere heats the snow surface, the surface temperature eventually reaches the freezing point and the snow and ice melting sets in. This process is accompanied by a consumption of heat at rates $L_f d\rho_s H_S/dt$ and $L_f d\rho_i H_I/dt$ for snow and ice, respectively. Notice that the exact form of the normalization function f_M is not required by virtue of the normalization conditions given above. Integrating Eq. (25) from $z = -(H_I + H_S) - 0$ to $z = -H_I$ with due regard for the heat loss due to snow melting and adding the (given) rate of snow accumulation yields the equation for the snow thickness,

$$L_f \frac{d\rho_s H_S}{dt} = -(Q_s + I_s) + I(-H_I) + L_f \left(\frac{dM_S}{dt}\right)_a + c_s \theta_f H_S \frac{d\rho_s}{dt}, \tag{51}$$

where the last term on the r.h.s. originates from the dependence of the snow density on the snow depth (see section 3.5.3).

Integrating Eq. (25) from $z = -H_I$ to $z = +0$ with due regard for the heat loss due to ice melting yields the equation for the ice thickness,

$$L_f \frac{d\rho_i H_I}{dt} = Q_w + I(0) - I(-H_I), \tag{52}$$

If the ice melts out earlier than snow, the snow depth is instantaneously set to zero.

3.4.3 The Temperature Profile beneath the Ice

The simplest assumption is to keep the temperature profile unchanged over the entire period of ice cover. This assumption is fair for deep lakes, where the heat flux through the bottom is negligibly small. In shallow lakes, this assumption may lead to an underestimation of the mean temperature. The heat accumulated in the thermally active upper layer of bottom sediments during spring and summer is returned back to the water column during winter, leading to an increase of the water temperature under the ice. The water temperature under the ice can also increase due to heating by solar radiation penetrating down through the ice. The thermodynamic regimes encountered in ice-covered lakes are many and varied. Their detailed description requires a set of sophisticated parameterizations. The use of such parameterizations in the framework of our lake model is, however, hardly justified. The point is that it is the snow (ice) surface temperature that communicates information to the atmosphere, the water temperature is not directly felt by the atmospheric surface layer. It is, therefore, not vital that the temperature regimes in ice-covered lakes be described in great detail. Only their most salient features should be accounted for, first of all, the heat budget of the water column.

When the lake is ice-covered, the temperature at the ice-water interface is fixed at the freezing $\theta_s = \theta_f$. In case the bottom temperature is less than the temperature of maximum density, $\theta_b < \theta_r$, the mixed-layer depth and the shape factor are kept unchanged, $dh/dt = 0$ and $dC_\theta/dt = 0$, the mean temperature $\overline{\theta}$ is computed from Eq. (26) and the bottom temperature θ_b is computed from Eq. (23). If the entire water column appears to be mixed at the moment of freezing, i.e. $h = D$ and $\theta_s = \overline{\theta} = \theta_b$, the mixed layer depth is reset to zero, $h = 0$, and the shape factor is set to its minimum value, $C_\theta = 0.5$ (see section 3.5.1). The heat flux from water to ice is estimated from

$$Q_w = -\kappa_w \frac{\theta_b - \theta_s}{D}, \tag{53}$$

if $h = 0$, and $Q_w = 0$ otherwise. Here, κ_w is the molecular heat conductivity of water. Notice that the estimate of Q_w given by Eq. (53) and the shape factor $C_\theta = 0.5$ correspond to a linear temperature profile over the entire water column. A linear profile is encountered in ice-covered shallow lakes when $\theta_b < \theta_r$ and heat flows from the bottom sediments to the water column.

As the bottom temperature reaches the temperature of maximum density, convection due to bottom heating sets in. To describe this regime of convection in detail, a convectively mixed layer whose temperature is close to θ_r, and a thin layer adjacent to the bottom, where the temperature decreases sharply from $\theta_b > \theta_r$ to θ_r, should be thoroughly considered. We neglect these peculiarities of convection due to bottom heating and adopt a simpler model where the bottom temperature is fixed at the temperature of maximum density, $\theta_b = \theta_r$. The mean temperature $\overline{\theta}$ is computed from Eq. (26). If $h > 0$, the shape factor C_θ is kept unchanged, and the mixed-layer depth is computed from Eq. (23). As the mixed-layer depth

approaches zero, Eq. (23) is used to compute the shape factor C_θ that in this regime increases towards its maximum value C_θ^{max}. The heat flux from water to ice is estimated from

$$Q_w = -\kappa_w \frac{\theta_b - \theta_s}{D} \max\left[1, \Phi'_\theta(0)\right], \tag{54}$$

if $h = 0$, and $Q_w = 0$ otherwise.

One more regime of convection is often encountered in ice-covered lakes. In late spring, the snow overlying the ice vanishes and solar radiation penetrates down through the ice. As the mixed-layer temperature is below that of maximum density, the volumetric radiation heating leads to de-stabilisation of the water column and thereby drives convective motions. Such regime of convection was analysed by Farmer (1975), Mironov and Terzhevik (2000), Mironov et al. (2002) and Jonas et al. (2003), among others. A parameterization of convection due to solar heating (e.g. a parameterization based on a bulk model developed by Mironov et al. 2002) can, in principle, be incorporated in our lake model. We do not do so, however, considering that the major effect of convection in question is to redistribute heat in the vertical and that it takes place over a very limited period of time.

3.5 Empirical Relations and Model Constants

3.5.1 The Shape Functions

In the lake model proposed by Mironov et al. (1991), a polynomial approximation of the shape function with respect to the temperature profile in the thermocline was used. The temperature-depth curve was assumed to be bounded by the two limiting curves given by Eq. (5). The shape function $\Phi_\theta(\zeta)$ evolves towards the first line of Eq. (5) during the mixed-layer deepening, and towards the second line of Eq. (5) during the mixed-layer stationary state or retreat. The corresponding limiting values of the shape factor C_θ are 0.75 and 0.6, respectively. The adjustment of the temperature-depth curve occurs on a certain relaxation time scale that was estimated on the basis of the similarity theory for stably stratified turbulent flows (see Mironov et al. 1991 for details).

Recall that the approximations (5) are based on the observational data taken in the Baltic Sea. Theoretical analysis of Zilitinkevich et al. (1988) also holds for the ocean or sea, where the thermocline is underlain by a deep quiescent layer. Shallow and medium-depth lakes usually have a two-layer temperature structure, where the thermocline extends from the bottom of the mixed layer down to the basin bottom. Empirical data indicate a greater variety of shapes of the temperature-depth curve in lakes than in the ocean or sea (Kirillin 2001a,b). During the mixed-layer deepening, the dimensionless temperature gradient just below the mixed layer-thermocline interface and the shape factor often exceed their limiting values of $\Phi'_\theta(0) = 3$ and $C_\theta = 0.75$, respectively, suggested by the first line of Eq. (5). These findings are corroborated by the theoretical analysis in Appendix A. Based upon these empirical and theoretical findings, we allow a wider range of variation in Φ_θ.

We adopt the following polynomial approximation of the shape function $\Phi_\theta(\zeta)$ with respect to the temperature profile in the thermocline:

$$\Phi_\theta = \left(\frac{40}{3}C_\theta - \frac{20}{3}\right)\zeta + (18 - 30C_\theta)\,\zeta^2 + (20C_\theta - 12)\,\zeta^3 + \left(\frac{5}{3} - \frac{10}{3}C_\theta\right)\zeta^4. \tag{55}$$

The shape factor C_θ is computed from

$$\frac{dC_\theta}{dt} = \mathrm{sign}(dh/dt)\frac{C_\theta^{max} - C_\theta^{min}}{t_{rc}}, \qquad C_\theta^{min} \le C_\theta \le C_\theta^{max}, \tag{56}$$

where t_{rc} is the relaxation time scale, and sign is the signum function, sign(x)=-1 if $x \le 0$ and sign(x)=1 if $x > 0$. The minimum and maximum values of the shape factor are set to $C_\theta^{min} = 0.5$ and $C_\theta^{max} = 0.8$. The shape functions $\Phi_\theta(\zeta)$ given by Eq. (55) are illustrated in Fig. 4. As seen from the figure, the dimensionless temperature profiles lie in the area bounded by the lower and the upper solid curves. During the mixed-layer deepening, $dh/dt > 0$, the temperature profile evolves towards the limiting curve, characterised by a maximum value of the shape factor, $C_\theta^{max} = 0.8$, and the maximum value of the dimensionless temperature gradient at the upper boundary of the thermocline, $\Phi'_\theta(0) = 4$. During the mixed-layer stationary state or retreat, $dh/dt \le 0$, the temperature profile evolves towards the other limiting curve, characterised by a minimum value of the shape factor, $C_\theta^{min} = 0.5$, and the zero temperature gradient at the upper boundary of the thermocline, $\Phi'_\theta(0) = 0$. Notice that $C_\theta^{min} = 0.5$ is consistent with a linear temperature profile that is assumed to occur under the ice when the bottom temperature is less than the temperature of maximum density (see section 3.4.3). According to Eq. (55), the dimensionless parameter $C_{\theta\theta}$ defined through Eq. (31) is given by

$$C_{\theta\theta} = \frac{11}{18} C_\theta - \frac{7}{45}. \tag{57}$$

The relaxation time t_{rc} is estimated from the following scaling arguments. The time t_{rc} is basically the time of the evolution of the temperature profile in the thermocline from one limiting curve to the other, following the change of sign in dh/dt. Then, a reasonable scale for t_{rc} is the thermal diffusion time through the thermocline, that is a square of the thermocline thickness, $(D-h)^2$, over a characteristic eddy temperature conductivity, K_{H*}. With due regard for the stable stratification in the thermocline, K_{H*} is estimated from Eqs. (14) and (16). Using a mean-square buoyancy frequency in the thermocline, $\overline{N} = \left[(D-h)^{-1} \int_h^D N^2 dz\right]^{1/2}$, as an estimate of N and assuming that the TKE in the thermocline scales either on the convective velocity w_*, Eq. (34), or on the surface friction velocity u_*, we propose

$$t_{rc} = \frac{(D-h)^2 \overline{N}}{C_{rc} u_T^2}, \qquad u_T = \max(w_*, u_*), \tag{58}$$

where C_{rc} is a dimensionless constant tentatively estimated at 0.003.

We adopt the following polynomial approximations of the shape functions $\Phi_{B1}(\zeta_{B1})$ and $\Phi_{B2}(\zeta_{B2})$ with respect to the temperature profile in bottom sediments (cf. Golosov et al. 1998):

$$\Phi_{B1} = 2\zeta_{B1} - \zeta_{B1}^2, \qquad \Phi_{B2} = 6\zeta_{B2}^2 - 8\zeta_{B2}^3 + 3\zeta_{B2}^4. \tag{59}$$

which are the simplest polynomials that satisfy a minimum set of constraints. The conditions $\Phi_{B1}(0) = \Phi_{B2}(0) = 0$ and $\Phi_{B1}(1) = \Phi_{B2}(1) = 1$ follow from the definition of ζ_{B1}, ζ_{B2}, Φ_{B1} and Φ_{B2}. The conditions $\Phi'_{B1}(1) = \Phi'_{B2}(0) = \Phi'_{B2}(1) = 0$ provide a zero temperature gradient at the depths $z = H$ and $z = L$, and the condition $\Phi''_{B2}(1) = 0$ follows from the requirement that the temperature θ_L at the outer edge $z = L$ of the thermally active layer of the sediments is constant in time. The shape functions given by Eq. (59) are illustrated in Fig. 5. The shape factors that correspond to Eq. (59) are $C_{B1} = 2/3$ and $C_{B2} = 3/5$.

As a zero-order approximation, the simplest linear temperature profile within snow and ice can be assumed, $\Phi_S(\zeta_S) = \zeta_S$ and $\Phi_I(\zeta_I) = \zeta_I$. This gives $C_S = C_I = 1/2$. Although a linear profile is a good approximation for thin ice, it is likely to result in a too thick ice in cold regions, where the ice growth takes place over a long period, and in a too high thermal

inertia of thick ice. A slightly more sophisticated approximation was developed by Mironov and Ritter (2004) who assumed that the ice thickness is limited by a certain maximum value H_I^{max} and that the rate of ice grows approaches zero as H_I approaches H_I^{max} (the snow layer over the ice was not considered). They proposed

$$\Phi_I = \left[1 - \frac{H_I}{H_I^{max}}\right] \zeta_I + \left[(2 - \Phi_{*I}) \frac{H_I}{H_I^{max}}\right] \zeta_I^2 + \left[(\Phi_{*I} - 1) \frac{H_I}{H_I^{max}}\right] \zeta_I^3, \tag{60}$$

where Φ_{*I} is a dimensionless constant. The shape factor that correspond to Eq. (60) is

$$C_I = \frac{1}{2} - \frac{1}{12}(1 + \Phi_{*I}) \frac{H_I}{H_I^{max}}. \tag{61}$$

The physical meaning of the above expressions can be elucidated as follows. The relation $\Phi_I'(0) = 1 - H_I/H_I^{max}$ that follows from Eq. (60) ensures that the ice growth is quenched as the ice thickness approaches its maximum value. Equation (61) suggests that the shape factor C_I decreases with increasing ice thickness. A smaller C_I means a smaller relative thermal inertia of the ice layer of thickness H_I [the absolute thermal inertia is measured by the term $C_I H_I$ that enters the l.h.s. of Eq. (46)]. This is plausible as it is mostly the upper part of thick ice, not the entire ice layer, that effectively responds to external forcing. For use in the global numerical weather prediction system GME of the German Weather Service, Mironov and Ritter (2004) proposed an estimate of $H_I^{max} = 3$ m. This value is typical of the central Arctic in winter. The allowable values of Φ_{*I} lie in the range between -1 and 5. $\Phi_{*I} > 5$ yields an unphysical negative value of C_I as the ice thickness approaches H_I^{max}. $\Phi_{*I} < -1$ gives C_I that increases with increasing H_I. There is no formal proof that this may not occur, but it is very unlikely. A reasonable estimate is $\Phi_{*I} = 2$. With this estimate C_I is halved as H_I increases from 0 to H_I^{max}. Notice that the linear temperature profile is recovered as $H_I/H_I^{max} \ll 1$, i.e. when the ice is thin. The polynomial (60) is illustrated in Fig. 6.

One further comment is in order regarding the shape functions Φ_θ, Φ_{B1}, Φ_{B2}, Φ_S and Φ_I. These functions have been determined using a geometrical approach (the Polhausen method). The essence of the approach is to use a polynomial approximation of the function in question and to invoke a minimum set of physical constraints to determine the polynomial coefficients. In spite of the utter simplicity of this approach, it often yields very accurate results. Prominent examples are the boundary-layer similarity models developed by Long (1974) and Zilitinkevich (1989a, 1989b). Notice finally that, although the shape functions are useful in that they provide a continuous temperature profile trough the snow, ice, water and bottom sediments, their exact shapes are not required in our model. It is not $\Phi_\theta(\zeta)$, $\Phi_{B1}(\zeta_{B1})$, $\Phi_{B2}(\zeta_{B2})$, $\Phi_S(\zeta_S)$ and $\Phi_I(\zeta_I)$ per se, but the shape factors C_θ, C_{B1}, C_{B2}, C_S and C_I, and the dimensionless gradients $\Phi_\theta'(0)$, $\Phi_{B1}'(0)$, $\Phi_S'(0)$, $\Phi_I'(0)$ and $\Phi_I'(1)$, that enter the model equations. The estimates of these parameters are summarised in Table 1.

3.5.2 Constants in the Equations for the Mixed-Layer Depth

The estimates of $C_{c1} = 0.2$ and $C_{c2} = 0.8$ in Eq. (35) were recommended by Zilitinkevich (1991). They were obtained using laboratory, atmospheric and oceanic data. Apart from being commonly used in mixed-layer models of penetrative convection driven by the surface buoyancy flux, these values were successfully used by Mironov and Karlin (1989) to simulate day-time convection in the upper ocean that is driven by surface cooling but inhibited by radiation heating, and by Mironov and Terzhevik (2000) and Mironov et al. (2002) to simulate spring convection in ice-covered lakes, where convective motions are driven by volumetric radiation heating of the water at temperature below the temperature of maximum density

(Mironov et al. 2002 used $C_{c2} = 1.0$). A slightly modified estimate of $C_{c1} = 0.17$ was obtained by Fedorovich et al. (2003) from large-eddy simulation data. We adopt the estimates of $C_{c1} = 0.17$ and $C_{c2} = 1.0$ for use in the equation of convective entrainment.

For use in Eq. (38) for the equilibrium mixed-layer depth in stable or neutral stratification, we adopt the estimates of $C_n = 0.5$, $C_s = 10$ and $C_i = 20$ obtained by Zilitinkevich and Mironov (1996). The estimates of C_s and C_i are based on a limited amount of data and may need to be slightly altered as new (and better) data become available. The estimate of C_n was corroborated by the results from further studies (Zilitinkevich and Esau 2002, 2003) and is reliable.

The estimates of the dimensionless constant C_{rh} in the relaxation-type rate equation for the depth of a stably or neutrally stratified wind-mixed layer, Eqs. (36) and (37), are not abundant. Kim (1976) and Deardorff (1983) recommended that the value of $C_{rh} = 0.28$ be used to describe entrainment into a homogeneous fluid. The same value was used by Zeman (1979), and a slightly lower value of $C_{rh} = 0.26$, by Zilitinkevich et al. (1979). The rate equations given by Khakimov (1976) and Zilitinkevich et al. (2002a) use the reciprocal of the Coriolis parameter as the relaxation time scale. Their rate equations suggest the values of $C_{rh} = 0.45$ and $C_{rh} = 0.5$, respectively. A similar form of the rate equation was proposed earlier by Deardorff (1971) who used a much lower value of $C_{rh} = 0.025$. We adopt an estimate of $C_{rh} = 0.01$ suggested by the sensitivity experiments with the proposed lake model, keeping in mind that this tentative value may need to be altered.

The estimates of dimensionless constants in the equations for the mixed-layer depth are summarised in Table 1.

3.5.3 Thermodynamic Parameters

The model includes a number of thermodynamic parameters. They are summarised in Table 2. These thermodynamic parameters can be considered constant except for the snow density and the snow heat conductivity that are functions of snow thickness and snow age. We adopt the following simplified empirical approximations (Heise et al. 2003), relating ρ_s and κ_s to the snow thickness:

$$\rho_s = \min\left\{\rho_s^{max}, |1 - H_S\Gamma_{\rho_s}/\rho_w|^{-1}\,\rho_s^{min}\right\}, \tag{62}$$

where $\rho_s^{min} = 100$ kg·m^{-3} and $\rho_s^{max} = 400$ kg·m^{-3} are minimum and maximum values, respectively, of the snow density, and $\Gamma_{\rho_s} = 200$ kg·m^{-4} is an empirical parameter; and

$$\kappa_s = \min\left\{\kappa_s^{max}, \kappa_s^{min} + H_S\Gamma_{\kappa_s}\rho_s/\rho_w\right\}, \tag{63}$$

where $\kappa_s^{min} = 0.2$ J·m^{-1}·s^{-1}·K^{-1} and $\kappa_s^{max} = 1.5$ J·m^{-1}·s^{-1}·K^{-1} are minimum and maximum values, respectively, of the snow heat conductivity, and $\Gamma_{\kappa_s} = 1.3$ J·m^{-2}·s^{-1}·K^{-1} is an empirical parameter. The above approximations are currently used in the operational NWP system of the German Weather Service.

The exponential approximation of the decay law for the flux of short-wave radiation is commonly used in applications. It reads

$$I(t,z) = I_s(t)\sum_{k=1}^{n} a_k \exp[-\gamma_k(z + H_S + H_I)], \tag{64}$$

where I_s is the surface value of the short-wave radiation heat flux multiplied by $1 - \alpha$, α being the albedo of the water, ice or snow surface with respect to short-wave radiation, n

is the number of wavelength bands, a_k are fractions of the total radiation flux for different wavelength bands, and $\gamma_k(z)$ are attenuation coefficients for different bands. The attenuation coefficients are piece-wise constant functions of height, i.e. they have different values for water, ice and snow but remain height-constant within these media. The optical characteristics of water are lake-specific and should be estimated with caution in every particular case. Rough estimates of a_k and γ_k for ice and snow are given by Launiainen and Cheng (1998).

4 Conclusions

We have developed a lake model suitable to predict the vertical temperature structure in lakes of various depths on time scales from a few hours to a year. The model is based on a two-layer parameterization of the temperature profile, where the structure of the stratified layer between the upper mixed layer and the basin bottom, the lake thermocline, is described using the concept of self-similarity of the evolving temperature profile. The same concept is used to describe the interaction of the water column with bottom sediments and the evolution of the ice and snow cover. The proposed lake model should be tested against observational data through single-column numerical experiments. The results will be presented in a companion paper (Part 2).

The lake model described above contains a number of dimensionless constants and empirical parameters. Most of them have been estimated with a fair degree of confidence. The exceptions are the constants C_{rh} and C_{rc} in the relaxation-type equations for the depth of a wind-mixed layer and for the shape factor with respect to the temperature profile in the thermocline, respectively. Only tentative estimates of these constants have been given that may need to be altered. It must be emphasised that the empirical constants and parameters of the lake model are not application-specific. That is, once they have been estimated, using independent empirical and numerical data, they should not be re-evaluated when the model is applied to a particular lake. In this way we avoid "tuning", a procedure that may improve an agreement with a limited amount of data and is sometimes justified. This procedure should, however, be considered as a bad practice and must be avoided whenever possible as it greatly reduces the predictive capacity of a physical model (Randall and Wielicki 1997).

Apart from the optical characteristics of lake water, the only lake-specific parameters are the lake depth D, the depth L of the thermally active layer of bottom sediments and the temperature θ_L at this depth. These parameters should be estimated only once for each lake, using observational data or empirical recipes (e.g. Fang and Stefan 1998). In a similar way, the temperature at the bottom of the thermally active soil layer and the depth of this layer are estimated once and then used in an NWP system as two-dimensional external parameter arrays.

The proposed lake model is intended for use, first of all, in NWP and climate modelling systems as a module to predict the water surface temperature. Apart from NWP and climate modelling, practical applications, where simple bulk models are favoured over more accurate but more sophisticated models (e.g. second-order turbulence closures), include modelling aquatic ecosystems. For ecological modelling, a sophisticated physical module is most often not required because of insufficient knowledge of chemistry and biology.

Acknowledgements

The work was partially supported by the EU Commissions through the project INTAS-01-2132.

Appendix A. Temperature Profile in the Lake Thermocline – A Self-Similar Travelling Wave-Type Solution

In section 2.3, we have discussed a travelling wave-type self-similar solution to the heat transfer equation obtained by Zilitinkevich et al. (1988). These authors analysed the heat transfer equation in the form

$$\partial\theta/\partial t = -\partial\mathcal{Q}/\partial z, \tag{A.1}$$

where $\mathcal{Q}$ is the vertical turbulent temperature flux, subject to the boundary conditions

$$\theta = \theta_s \quad \text{at} \quad z = h, \qquad \theta = \theta_b \quad \text{at} \quad z = h + \Delta h. \tag{A.2}$$

They assumed that the temperatures at the upper and lower boundaries of the thermocline are constant, $\theta_s = const$ and $\theta_b = const$, the mixed layer deepens at a constant rate, $dh/dt \equiv \dot{h} = const > 0$, whereas the thickness of the thermocline does not change with time, $d\Delta h/dt = 0$. Then, the heat transfer equation (A.1) takes the form

$$\dot{h} d\theta/d\zeta = d\mathcal{Q}/d\zeta, \tag{A.3}$$

where $\zeta = (z-h)/\Delta h$ is the dimensionless depth. In order to close the problem, Zilitinkevich et al. (1988) used the down-gradient formulation for the temperature flux, $\mathcal{Q} = -K_H \partial\theta/\partial z$, and the expression $K_H = l^2 N$ for the effective temperature conductivity in the thermocline, where l is the eddy length scale. Taking $l = const$, they invoked an additional condition $\partial\theta/\partial z = 0$ at $z = h + \Delta h$ to determine l. The solution to the problem reads

$$\Phi_\theta = 1 - (1-\zeta)^3, \qquad l = 3^{-3/4}(\beta\Delta\theta)^{-1/4}\Delta h^{3/4}\dot{h}^{1/2}. \tag{A.4}$$

The temperature profile shape function Φ_θ is given by the third-order polynomial in ζ. This polynomial was developed earlier by Arsenyev and Felzenbaum (1977) from simple geometrical arguments and by Mälkki and Tamsalu (1985) on the basis of data from measurements in the Baltic Sea.

The Zilitinkevich et al. (1988) solution (A.4) is conditioned by the assumption $d\Delta h/dt = 0$. This situation is illustrated in Fig. 7(a). It is characteristic of the ocean or sea, where the mixed layer grows into a neutrally stratified deep quiescent layer, whereas the thickness of the thermocline remains approximately unchanged. In lakes, the thermocline is usually pressed against the basin bottom so that an increase of the mixed-layer thickness is accompanied by a decrease of the thickness of the thermocline, $dh/dt = -d\Delta h/dt$. This situation is illustrated in Fig. 7(b). With $dh/dt = -d\Delta h/dt = const > 0$, the heat transfer equation (A.1) takes the form

$$\dot{h}(1-\zeta) d\theta/d\zeta = d\mathcal{Q}/d\zeta. \tag{A.5}$$

It is easy to verify that Eq. (A.5) subject to the same boundary conditions and closure relations as used by Zilitinkevich et al. (1988) possesses a solution in the form

$$\Phi_\theta = 1 - (1-\zeta)^5, \qquad l = 180^{-1/4}(\beta\Delta\theta)^{-1/4}\Delta h^{3/4}\dot{h}^{1/2}. \tag{A.6}$$

Equations (A.4) and (A.6) reveal a number of differences between the lake thermocline that is pressed against the bottom and the ocean thermocline that is underlain by a deep neutrally stratified quiescent layer. The eddy length scale l characteristic of the lake thermocline is $(20/3)^{1/4}$ times smaller than l characteristic of the ocean thermocline. The temperature

profile in the lake thermocline is characterised by a sharper temperature gradient near the thermocline top. The dimensionless temperature gradients at the top of the thermocline, $-(\Delta\theta/\Delta h)^{-1}(\partial\theta/\partial z)|_{z=h} \equiv \Phi'_\theta(0)$, $\Delta\theta = \theta_s - \theta_b$ being the temperature difference across the thermocline, are $\Phi'_\theta(0) = 5$ for the lake and $\Phi'_\theta(0) = 3$ for the ocean. The temperature profile shape factor is $C_\theta = 5/6$ for the lake and $C_\theta = 3/4$ for the ocean.

As Eq. (A.3) suggests, the self-similar oceanic thermocline is characterised by the shape function $\Phi_\theta \equiv (\theta_s - \theta)/(\theta_s - \theta_b)$ with respect to the temperature that coincides with the shape function $\Phi_Q \equiv (\mathcal{Q}_h - \mathcal{Q})/(\mathcal{Q}_h - \mathcal{Q}_b)$ with respect to the temperature (heat) flux. For the lake thermocline, the relation between Φ_θ and Φ_Q is more sophisticated. Equation (A.5) yields

$$\Phi_Q(\zeta) = C_\theta^{-1}\left[(1-\zeta)\Phi_\theta(\zeta) + \int_0^\zeta \Phi_\theta(\zeta')d\zeta'\right]. \tag{A.7}$$

The above relation suggests that the dimensionless shape-function parameters C_Q, $C_{\theta\theta}$ and C_θ defined by Eqs. (30), (31) and (24), respectively, are related through $C_Q = 2C_{\theta\theta}/C_\theta$.

Appendix B. A Summary of Model Parameters

Table 1: Empirical Constants and Parameters

Constant/ Parameter	Recommended Value/ Computed from	Comments
C_{c1}	0.17	
C_{c2}	1.0	
C_n	0.5	
C_s	10	
C_i	20	
C_{rh}	0.03	
C_{rc}	0.003	
C_θ	Eq. (56)	
C_θ^{min}	0.5	
C_θ^{max}	0.8	
$C_{\theta\theta}$	Eq. (57)	
C_Q	$2C_{\theta\theta}/C_\theta$	
C_{B1}	2/3	
C_{B2}	3/5	
C_I	1/2	Optionally Eq. (61)
C_S	1/2	
$\Phi'_\theta(0)$	Eqs. (55) and (56)	
$\Phi'_{B1}(0)$	2	
$\Phi'_I(0)$	1	Optionally Eq. (60)
$\Phi'_I(1)$	1	Optionally Eq. (60)
$\Phi'_S(0)$	1	
Φ_{*I}	2	
H_I^{max}	3 m	

Table 2: Thermodynamic Parameters

Notation	Parameter	Dimensions	Estimate/ Computed from
g	Acceleration due to gravity	$\mathrm{m{\cdot}s^{-2}}$	9.81
θ_r	Temperature of maximum density of fresh water	K	277.13
θ_f	Fresh water freezing point	K	273.15
a_T	Coefficient in the fresh-water equation of state	$\mathrm{K^{-2}}$	$1.6509 \cdot 10^{-5}$
ρ_w	Density of fresh water	$\mathrm{kg{\cdot}m^{-3}}$	Eq. (20)
ρ_r	Maximum density of fresh water	$\mathrm{kg{\cdot}m^{-3}}$	$1.0 \cdot 10^3$
ρ_i	Density of ice	$\mathrm{kg{\cdot}m^{-3}}$	$9.1 \cdot 10^2$
ρ_s	Density of snow	$\mathrm{kg{\cdot}m^{-3}}$	Eq. (62)
ρ_s^{min}	Minimum value of ρ_s	$\mathrm{kg{\cdot}m^{-3}}$	$1.0 \cdot 10^2$
ρ_s^{max}	Maximum value of ρ_s	$\mathrm{kg{\cdot}m^{-3}}$	$4.0 \cdot 10^2$
Γ_{ρ_s}	Empirical parameter, Eq. (62)	$\mathrm{kg{\cdot}m^{-4}}$	$2.0 \cdot 10^2$
L_f	Latent heat of fusion	$\mathrm{J{\cdot}kg^{-1}}$	$3.3 \cdot 10^5$
c_w	Specific heat of water	$\mathrm{J{\cdot}kg^{-1}{\cdot}K^{-1}}$	$4.2 \cdot 10^3$
c_i	Specific heat of ice	$\mathrm{J{\cdot}kg^{-1}{\cdot}K^{-1}}$	$2.1 \cdot 10^3$
c_s	Specific heat of snow	$\mathrm{J{\cdot}kg^{-1}{\cdot}K^{-1}}$	$2.1 \cdot 10^3$
κ_w	Molecular heat conductivity of water	$\mathrm{J{\cdot}m^{-1}{\cdot}s^{-1}{\cdot}K^{-1}}$	$5.46 \cdot 10^{-1}$
κ_i	Molecular heat conductivity of ice	$\mathrm{J{\cdot}m^{-1}{\cdot}s^{-1}{\cdot}K^{-1}}$	2.29
κ_s	Molecular heat conductivity of snow	$\mathrm{J{\cdot}m^{-1}{\cdot}s^{-1}{\cdot}K^{-1}}$	Eq. (63)
κ_s^{min}	Minimum value of κ_s	$\mathrm{J{\cdot}m^{-1}{\cdot}s^{-1}{\cdot}K^{-1}}$	0.2
κ_s^{max}	Maximum value of κ_s	$\mathrm{J{\cdot}m^{-1}{\cdot}s^{-1}{\cdot}K^{-1}}$	1.5
Γ_{κ_s}	Empirical parameter, Eq. (63)	$\mathrm{J{\cdot}m^{-2}{\cdot}s^{-1}{\cdot}K^{-1}}$	1.3

References

Abramowitz, M., and I. A. Stegun, 1964: *Handbook of Mathematical Functions.* National Bureau of Standards, Applied Mathematics Series 55.

Arsenyev, S. A., and A. I. Felzenbaum, 1977: Integral model of the active ocean layer. *Izv. Akad. Nauk SSSR. Fizika Atmosfery i Okeana*, **13**, 1034–1043.

Barenblatt, G. I., 1978: On the self-similar distribution of temperature and salinity in the upper thermocline. *Izv. Akad. Nauk SSSR. Fizika Atmosfery i Okeana*, **14**, 1160–1166.

Brost, R. A., and J. C. Wyngaard, 1978: A model study of the stably stratified planetary boundary layer. *J. Atmos. Sci.*, **35**, 1427–1440.

Deardorff, J. W., 1970a: Preliminary results from numerical integrations of the unstable planetary boundary layer. *J. Atmos. Sci.*, **27**, 1209–1211.

Deardorff, J. W., 1970b: Convective velocity and temperature scales for the unstable planetary boundary layer and for Rayleigh convection. *J. Atmos. Sci.*, **27**, 1211–1213.

Deardorff, J. W., 1971: Rate of growth of the nocturnal boundary layer. Paper presented at Symposium on Air Pollution, Turbulence and Diffusion, Las Cruces, N. M., NCAR ms. No. 71-246.

Deardorff, J. W., 1979: Prediction of convective mixed-layer entrainment for realistic capping inversion structure. *J. Atmos. Sci.*, **36**, 424–436.

Deardorff, J. W., 1983: A multi-limit mixed-layer entrainment formulation. *J. Phys. Oceanogr.*, **13**, 988–1002.

Efimov, S. S., and V. M. Tsarenko, 1980: On a self-similarity of the temperature distribution in the upper thermocline. *Izv. Akad. Nauk SSSR. Fizika Atmosfery i Okeana*, **16**, 620–627.

Ertel, H., 1954: Theorie der thermischen Sprungschiht in Seen. *Acta Hydrophys.*, Bd. 2, 151–171.

Fang, X., and H. G. Stefan, 1996: Dynamics of heat exchange between sediment and water in a lake. *Water Resour. Res.*, *32*, 1719–1727.

Fang, X., and H. G. Stefan, 1998: Temperature variability in lake sediments. *Water Resour. Res.*, *34*, 717–729.

Farmer, D. M., 1975: Penetrative convection in the absence of mean shear. *Quart. J. Roy. Meteorol. Soc.*, **101**, 869–891.

Farmer, D. M., and E. Carmack, 1981: Wind mixing and restratification in a lake near the temperature of maximum density. *J. Phys. Oceanogr.*, **11**, 1516–1533.

Fedorovich, E., R. Conzemius, and D. Mironov, 2004: Convective entrainment into a shear-free, lineraly stratified atmosphere: bulk models reevaluated through large eddy simulations. *J. Atmos. Sci.*, **61**, 281–295.

Fedorovich, E. E., and D. V. Mironov, 1995: A model for shear-free convective boundary layer with parameterized capping inversion structure. *J. Atmos. Sci.*, **52**, 83–95.

Filyushkin, B. N., and Yu. Z. Miropolsky, 1981: Seasonal variability of the upper thermocline and self-similarity of temperature profiles. *Okeanologia*, **21**, 416–424.

Golosov, S. D., and K. D. Kreiman, 1992: Heat exchange and thermal structure within "water-sediments" system. *Water Resources (Vodnye Resursy)*, **6**, 92–97.

Golosov, S., I. Zverev, and A. Terzhevik, 1998: *Modelling Thermal Structure and Heat Interaction between a Water Column and Bottom Sediments.* Report No. 3220 [LUTVDG/(TVVR-3220) 1-41(1998)], Dept. of Water Resources Engineering, Inst. of Technology, Univ. of Lund, Lund, Sweden, 41 p.

Goyette, S., N. A. McFarlane, and G. M. Flato, 2000: Application of the Canadian regional climate model to the Laurentian Great Lakes region: implementation of a lake model. *Atmosphere-Ocean*, **38**, 481–503.

Gu, R., and H. G. Stefan, 1990: Year-round temperature simulation of cold climate lakes. *Cold Reg. Sci. Technol.*, **18**, 147–160.

Heise, E., M. Lange, B. Ritter, and R. Schrodin, 2003: Improvement and validation of the multi-layer soil model. *COSMO Newsletter*, No. 3, Consortium for Small-Scale Modelling, Deutscher Wetterdienst, Offenbach am Main, Germany, 198-203. (available from www.cosmo-model.org)

Imberger, J., 1985: The diurnal mixed layer. *Limnol. Oceanogr.*, **30**, 737–770.

Jonas, T., A. Y. Terzhevik, D. V. Mironov, and A. Wüest, 2003: Investigation of radiatively-driven convection in an ice covered lake using temperature microstructure technique. *J. Geophys. Res.*, **108**, 14-1–14-18.

Kamenkovich, V. M., and B. V. Kharkov, 1975: On the seasonal variation of the thermal structure of the upper layer in the ocean. *Okeanologia*, **15**, 978–987.

Khakimov, I. R., 1976: The wind profile in the neutrally stratified atmospheric boundary layer. *Izv. Akad. Nauk SSSR. Fizika Atmosfery i Okeana*, **12**, 628–630.

Kharkov, B. V., 1977: On the structure of the upper ocean layer. *Okeanologia*, **17**, 37–43.

Kim, J.-W., 1976: A generalized bulk model of the oceanic mixed layer. *J. Phys. Oceanogr.*, **6**, 686–695.

Kirillin, G., 2001a: On self-similarity of thermocline in shallow lakes. *Proc. 6th Workshop on Physical Processes in Natural Waters*, X. Casamitjana, Ed., University of Girona, Girona, Spain, 221–225.

Kirillin, G., 2001b: On a self-similarity of the pycnocline. *Proc. 2001 International Symposium on Environmental Hydraulics*, Arizona State University, Tempe, Arizona, USA.

Kitaigorodskii, S. A., 1960: On the computation of the thickness of the wind-mixing layer in the ocean. *Izv. AN SSSR. Ser. geofiz.*, No. 3, 425–431.

Kitaigorodskii, S. A., 1970: *The Physics of Air-Sea Interaction.* Gidrometeoizdat, Leningrad, 284 p. (In Russian. English translation: Israel Progr. Scient. Translation, Jerusalem, 1973, 236 p.)

Kitaigorodskii, S. A., and S. M. Joffre, 1988: In search of simple scaling for the heights of the stratified atmospheric boundary layer. *Tellus*, **40A**, 419–433.

Kitaigorodskii, S. A., and Yu. Z. Miropolsky, 1970: On the theory of the open ocean active layer. *Izv. Akad. Nauk SSSR. Fizika Atmosfery i Okeana*, **6**, 178–188.

Kondratiev, S. A., S. D. Golosov, K. D. Kreiman, and N. V. Ignatieva, 1998: Modelling hydrological processes and mass transfer in a watershed-lake system. *Water Resources (Vodnye Resursy)*, **25**, 571–580.

Kraus, E. B., and C. Rooth, 1961: Temperature and steady state vertical heat flux in the ocean surface layer. *Tellus*, **13**, 231–238.

Launiainen, J., and B. Cheng, 1998: Modelling of ice thermodynamics in natural water bodies. *Cold. Reg. Sci. Technol.*, **27**, 153–178.

Leppäranta, M., 1993: A review of analytical models of sea-ice growth. *Atmosphere-Ocean*, **31**, 123–138.

Linden, P. F., 1975: The deepening of a mixed layer in a stratified fluid. *J. Fluid Mech.*, **71**, 385–405.

Ljungemyr, P., N. Gustafsson, and A. Omstedt, 1996: Parameterization of lake thermodynamics in a high-resolution weather forecasting model. *Tellus*, **48A**, 608–621.

Long, R. R., 1974: Mean stress and velocities in the neutral, barotropic planetary boundary layer. *Boundary-Layer Meteorol.*, **7**, 475–487.

Mälkki, P., and R. E. Tamsalu, 1985: Physical Features of the Baltic Sea. *Finnish Marine Research*, No. 252, Helsinki, 110 p.

Mironov, D. V., 1990: Calculating the temperature profile in a fresh-water thermocline. *Izv. Akad. Nauk SSSR. Fizika Atmosfery i Okeana*, **26**, 880–883.

Mironov, D. V., 1992: A one-dimensional parameterised model for the evolution of the temperature profile and mixing conditions in a lake. *Lake Ladoga – Criteria of the Ecosystem State*, N. A. Petrova and A. Yu. Terzhevik, Eds., "Nauka" Publishing House, St. Petersburg, 36–41.

Mironov, D. V., 1999: *The SUBMESO Meteorological Preprocessor. Physical Parameterisations and Implementation.* Technical Note, Laboratoire de Mécanique des Fluides UMR CNRS 6598, Ecole Centrale de Nantes, Nantes, France. 25 p.

Mironov, D. V., and E. Fedorovich, 2005: How important is the earth's rotation in limiting the depth of a stably stratified boundary layer? In preparation.

Mironov, D. V., S. D. Golosov, S. S. Zilitinkevich, K. D. Kreiman, and A. Yu. Terzhevik, 1991: Seasonal changes of temperature and mixing conditions in a lake. *Modelling Air-Lake Interaction. Physical Background*, S. S. Zilitinkevich, Ed., Springer-Verlag, Berlin, etc., 74–90.

Mironov, D. V., S. D. Golosov, and I. S. Zverev, 2003: Temperature profile in lake bottom sediments: an analytical self-similar solution. *Proc. 7th Workshop on Physical Processes in Natural Waters*, A. Yu. Terzhevik, Ed., Northern Water Problems Institute, Russian Academy of Sciences, Petrozavodsk, Karelia, Russia, 90–97.

Mironov, D. V., and L. N. Karlin, 1989: Penetrative convection due to surface cooling with vertically distributed heating. *Dokl. Akad. Nauk SSSR.*, **309**, 1336–1340.

Mironov, D., and B. Ritter, 2004: A New Sea Ice Model for GME. Technical Note, Deutscher Wetterdienst, Offenbach am Main, Germany, 12 p.

Mironov, D. V., and A. Yu. Terzhevik, 2000: Spring convection in ice-covered fresh-water lakes. *Izv. Akad. Nauk SSSR. Fizika Atmosfery i Okeana*, **36**, 627–634.

Mironov, D., A. Terzhevik, G. Kirillin, T. Jonas, J. Malm, and D. Farmer, 2002: Radiatively driven convection in ice-covered lakes: Observations, scaling, and a mixed layer model. *J. Geophys. Res.*, **107**, 7-1–7-16.

Miropolsky, Yu. Z., 1970: Non-stationary model of the wind-convection mixing layer in the ocean. *Okeanologia*, **6**, 1284–1294.

Miropolsky, Yu. Z., B. N. Filyushkin, and P. P. Chernyshkov, 1970: On the parametric description of temperature profiles in the active ocean layer. *Okeanologia*, **10**, 1101–1107.

Munk, W. H., and E. R. Anderson, 1948: Notes on a theory of the thermocline. *J. Marine Res.*, **7**, 276–295.

Nesterov, E. S., and V. I. Kalatsky, 1975: Parameterisation of the vertical temperature profile in the active layer in North Atlantic. *Trudy Gidrometzentra SSSR (Proc. Hydrometeorological Centre of the USSR)*, No. 161, 35–39.

Otte, M. J., and J. C. Wyngaard, 2001: Stably stratified interfacial-layer turbulence from large-eddy simulation. *J. Atmos. Sci.*, **58**, 3424–3442.

Pénelon, T., I. Calmet, and D. V. Mironov, 2001: Micrometeorological simulation over a complex terrain with SUBMESO: a model study using a novel pre-processor. *Int. J. Envir. and Pollution*, **16**, 583–602.

Pollard, R. T., P. B. Rhines, and R. O. R. Y. Thompson, 1973: The deepening of the wind-mixed layer. *Geophys. Fluid Dyn.*, **3**, 381–404.

Price, J. F., R. A. Weller, and R. Pinkel, 1986: Diurnal cycling: observations and models of the upper ocean response to diurnal heating. *J. Geophys. Res.*, **91**, 8411–8427.

Randall, D. A., and B. A. Wielicki, 1997: Measurements, models, and hypotheses in the atmospheric sciences. *Bull. Amer. Met. Soc.*, **78**, 399–406.

Reshetova, O. V., and D. V. Chalikov, 1977: On the universal structure of the active layer in the ocean. *Okeanologia*, **17**, 774–777.

Rossby, C. G., and R. B. Montgomery, 1935: The layer of frictional influence in wind and ocean currents. *Pap. Phys. Oceanogr. Meteorol.*, **3**, 1–101. (M.I.T. and Woods Hole Oceanogr. Inst.)

Ryanzhin, S. V., 1997: *Thermophysical Properties of Lake Sediments and Water-Sediments Heat Interaction.* Report No. 3214, Dept. of Water Resources Engineering, Inst. of Technology, Univ. of Lund, Lund, Sweden, 95 p.

Shapiro, G. I., 1980: Effect of fluctuations in the turbulent entrainment layer on the heat and mass transfer in the upper thermocline. *Izv. Akad. Nauk SSSR. Fizika Atmosfery i Okeana*, **16**, 433–436.

Soloviev, A. V., 1979: Fine thermal structure of the ocean surface layer in the POLYMODE-77 region. *Izv. Akad. Nauk SSSR. Fizika Atmosfery i Okeana*, **15**, 750–757.

Soloviev, A. V., and N. V. Vershinskii, 1982: The vertical structure of the thin surface layer of the ocean under conditions of low wind speed. *Deep-Sea Res.*, **29**, 1437–1449.

Stefan, J., 1891: Ueber die Theorie der Eisbildung, insbesondere über die Eisbildung im Polarmeere. *Ann. Phys.*, **42**, 269–286.

Tamsalu, R., and K. Myrberg, 1998: A theoretical and experimental study of the self-similarity concept. *MERI, Report Series of the Finnish Institute of Marine Research*, No. 37, 3–13.

Tamsalu, R., P. Mälkki, and K. Myrberg, 1997: Self-similarity concept in marine system modelling. *Geophysica*, **33**, 51–68.

Tsuang, B.-J., C.-Y. Tu, and K. Arpe, 2001: *Lake Parameterization for Climate Models.* Report No. 316, Max Planck Institute for Meteorology, Hamburg, March 2001, 72 p.

Turner, J. S., 1978: The temperature profile below the surface mixed layer. *Ocean Modeling*, No. 11, 6–8.

Voropaev, S. I., 1977: Laboratory modelling of the mixing process in a stratified fluid. *Proc. 1st Soviet Oceanography Congress*, Moscow, 20–25 June 1977, No. 1, *Oceanic Physics, Marine Technology*, p. 81.

Wyatt, L. R., 1978: Mixed layer development in an annular tank. *Ocean Modeling*, No. 17, 6–8.

Zeman, O., 1979: Parameterization of the dynamics of stable boundary layers and nocturnal jets. *J. Atmos. Sci.*, **36**, 792–804.

Zeman, O., and H. Tennekes, 1977: Parameterization of the turbulent energy budget at the top of the daytime atmospheric boundary layer. *J. Atmos. Sci.*, **34**, 111–123.

Zilitinkevich, S. S., 1972: On the determination of the height of the Ekman boundary layer. *Boundary-Layer Meteorol.*, **3**, 141–145.

Zilitinkevich, S. S., 1975: Comments on "A Model for the Dynamics of the Inversion Above a Convective Boundary Layer". *J. Atmos. Sci.*, **32**, 991–992.

Zilitinkevich, S. S., 1989a: Velocity profiles, resistance law and dissipation rate of mean flow kinetic energy in a neutrally and stably stratified planetary boundary layer. *Boundary-Layer Meteorol.*, **46**, 367–387.

Zilitinkevich, S. S., 1989b: Temperature profile and heat transfer law in neutrally and stably stratified planetary boundary layer. *Boundary-Layer Meteorol.*, **46**, 367–387.

Zilitinkevich, S. S., 1991: *Turbulent Penetrative Convection.* Avebury Technical, Aldershot, 179 p.

Zilitinkevich, S., and A. Baklanov, 2002: Calculation of the height of the stable boundary layer in practical applications. *Boundary-Layer Meteorol.*, **105**, 389–409.

Zilitinkevich, S., A. Baklanov, J. Rost, A.-S. Smedman, V. Lykosov, and P. Calanca, 2002a: Diagnostic and prognostic equations for the depth of the stably stratified Ekman boundary layer. *Quart. J. Roy. Meteorol. Soc.*, **128**, 25–46.

Zilitinkevich, S. S., D. V. Chalikov, and Yu. D. Resnyansky, 1979: Modelling the oceanic upper layer. *Oceanologica Acta*, **2**, 219–240.

Zilitinkevich, S., and I. Esau, 2002: On the integral measures of the neutral barotropic planetary boundary layer. *Boundary-Layer Meteorol.*, **104**, 371–379.

Zilitinkevich, S., and I. Esau, 2003: The effect of baroclinicity on the depth of neutral and stable planetary boundary layers. Accepted for publication in *Quart. J. Roy. Meteor. Soc.*

Zilitinkevich, S. S., E. E. Fedorovich, and D. V. Mironov, 1992: Turbulent heat transfer in stratified geophysical flows. *Recent Advances in Heat Transfer*, B. Sundén and A. Žukauskas, Eds., Elsevier Science Publisher B. V., Amsterdam, etc., 1123–1139.

Zilitinkevich, S. S., K. D. Kreiman, and A. I. Felzenbaum, 1988: Turbulence, heat exchange and self-similarity of the temperature profile in a thermocline. *Dokl. Akad. Nauk SSSR.*, **300**, 1226–1230.

Zilitinkevich, S. S., and D. V. Mironov, 1989: A theoretical model of thermocline evolution in a fresh-water basin. *Izv. Akad. Nauk SSSR. Fizika Atmosfery i Okeana*, **25**, 969–978.

Zilitinkevich, S. S., and D. V. Mironov, 1992: Theoretical model of the thermocline in a freshwater basin. *J. Phys. Oceanogr.*, **22**, 988–996.

Zilitinkevich, S. S., and D. V. Mironov, 1996: A multi-limit formulation for the equilibrium depth of a stably stratified boundary layer. *Boundary-Layer Meteorol.*, **81**, 325–351.

Zilitinkevich, S. S., V. L. Perov, and J. C. King, 2002b: Near-surface turbulent fluxes in stable stratification: Calculation techniques for use in general-circulation models. *Quart. J. Roy. Meteorol. Soc.*, **128**, 1571–1588.

Zilitinkevich, S. S., and V. A. Rumyantsev, 1990: A parameterized model of the seasonal temperature changes in lakes. *Environmental Software*, **5**, 12–25.

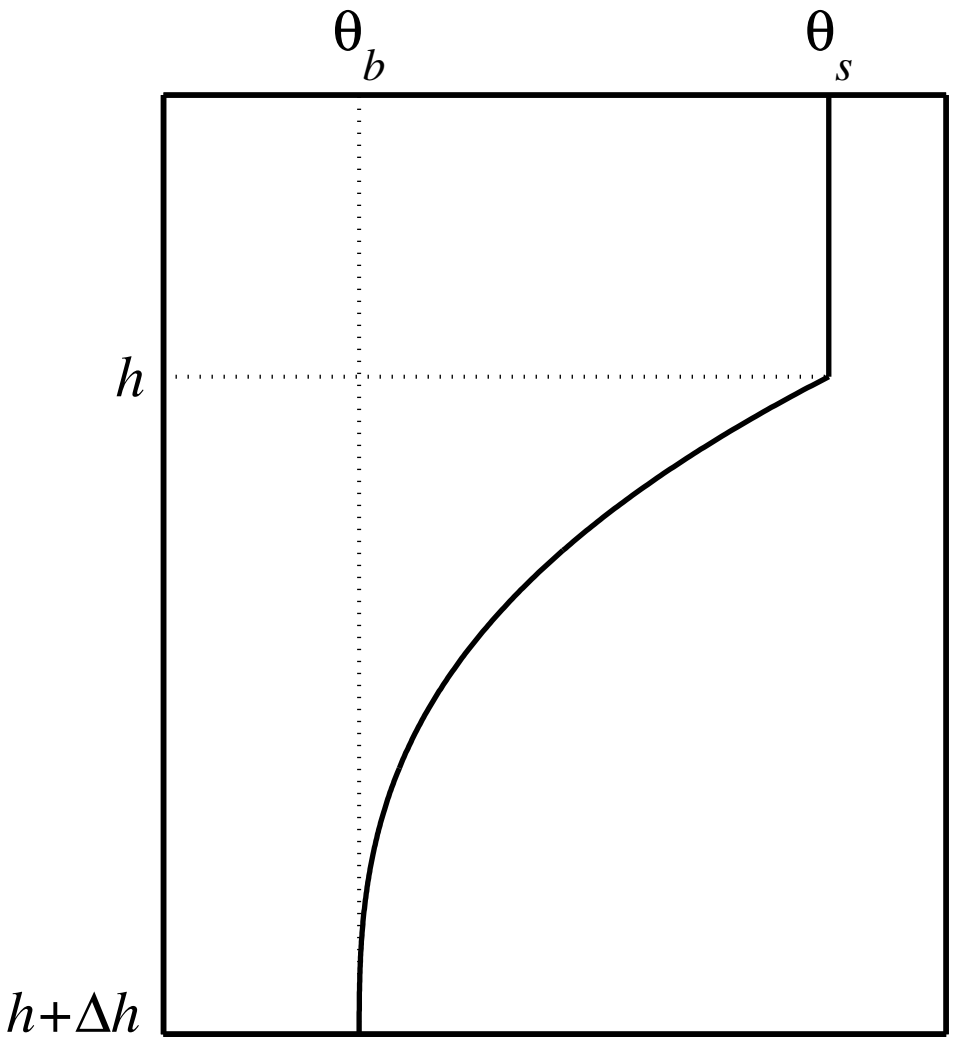

Figure 1. Schematic representation of the temperature profile in the upper mixed layer and in the thermocline. See text for notation.

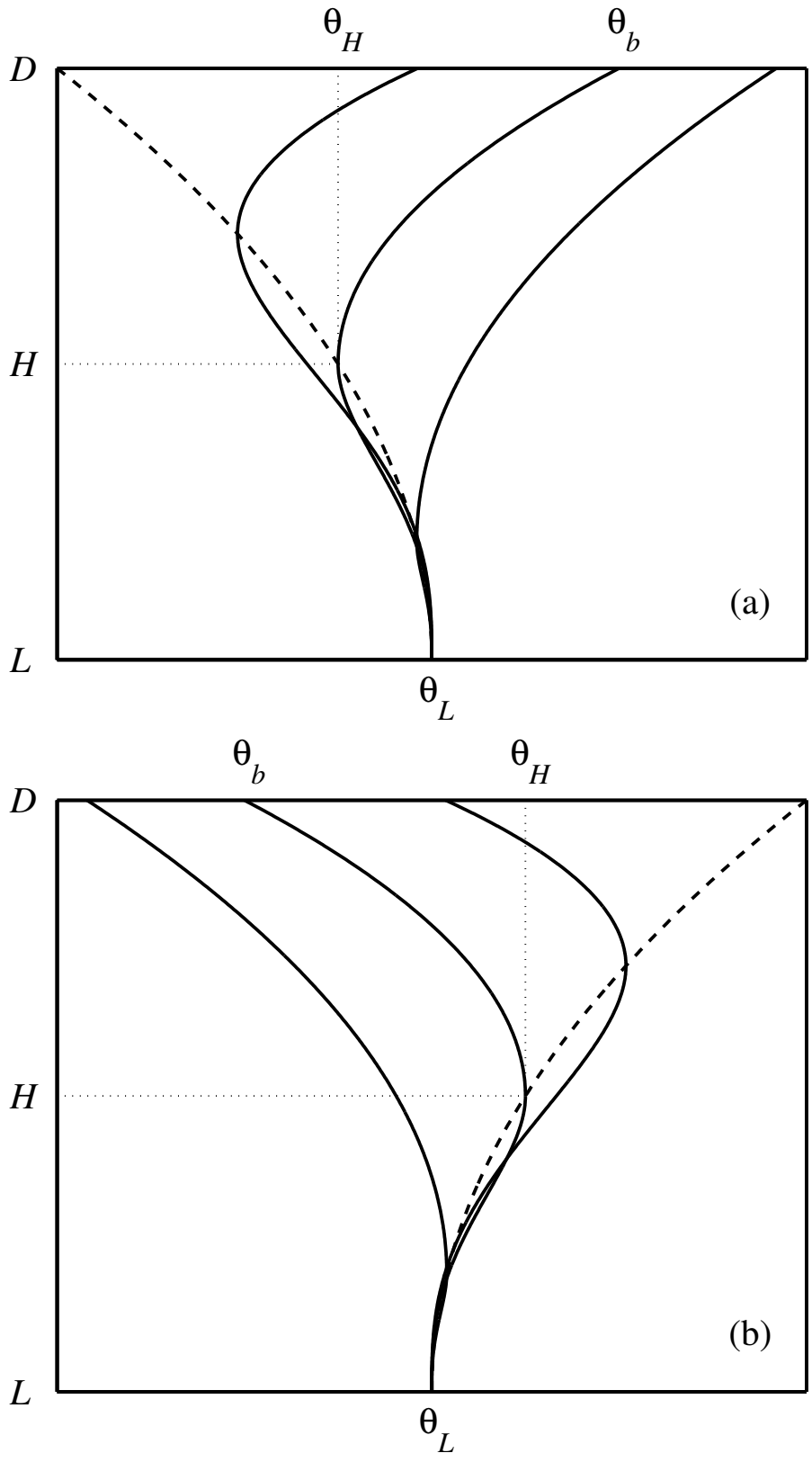

Figure 2. Schematic representation of the temperature profile in bottom sediments during periods of (a) heating and (b) cooling. Dashed curves show the initial temperature profiles, i.e. the profiles developed towards the end of the previous period of cooling (heating). See text for details.

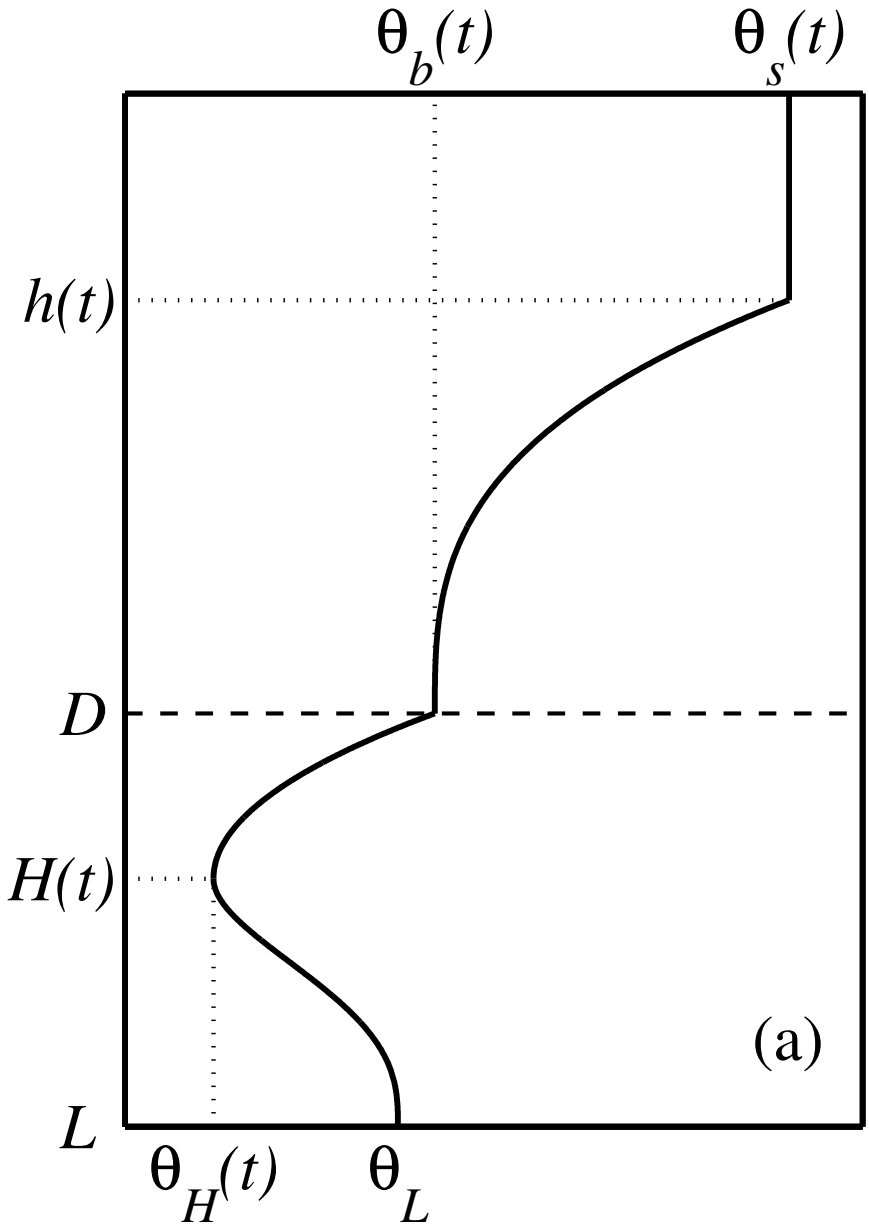

Figure 3. (a) Schematic representation of the temperature profile in the mixed layer, in the thermocline and in the thermally active layer of bottom sediments. The evolving temperature profile is specified by five time-dependent quantities, namely, the mixed-layer temperature $\theta_s(t)$ and its depth $h(t)$, the temperature $\theta_b(t)$ at the water-bottom sediment interface, the temperature $\theta_H(t)$ at the bottom of the upper layer of bottom sediments penetrated by the thermal wave, and the depth $H(t)$ of this layer. The temperature θ_L at the outer edge $z = L$ of the thermally active layer of the sediments is constant.

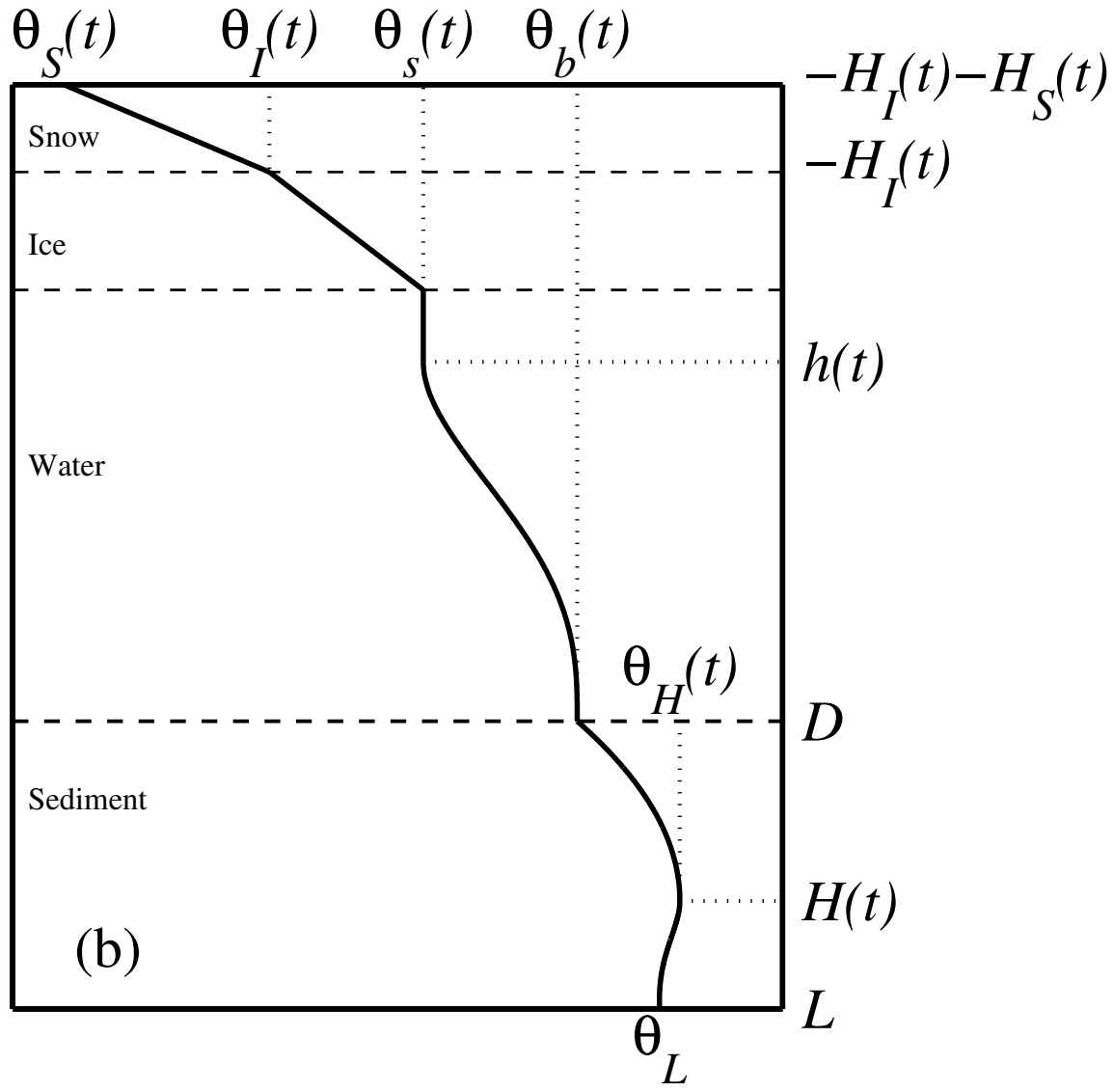

Figure 3. (continued). (b) In case the lake is covered by ice and snow, four additional quantities are computed, namely, the temperatures $\theta_S(t)$ at the air-snow interfaces, the temperatures $\theta_I(t)$ at the snow-ice interfaces, the snow depth $H_S(t)$ and the ice depth $H_I(t)$.

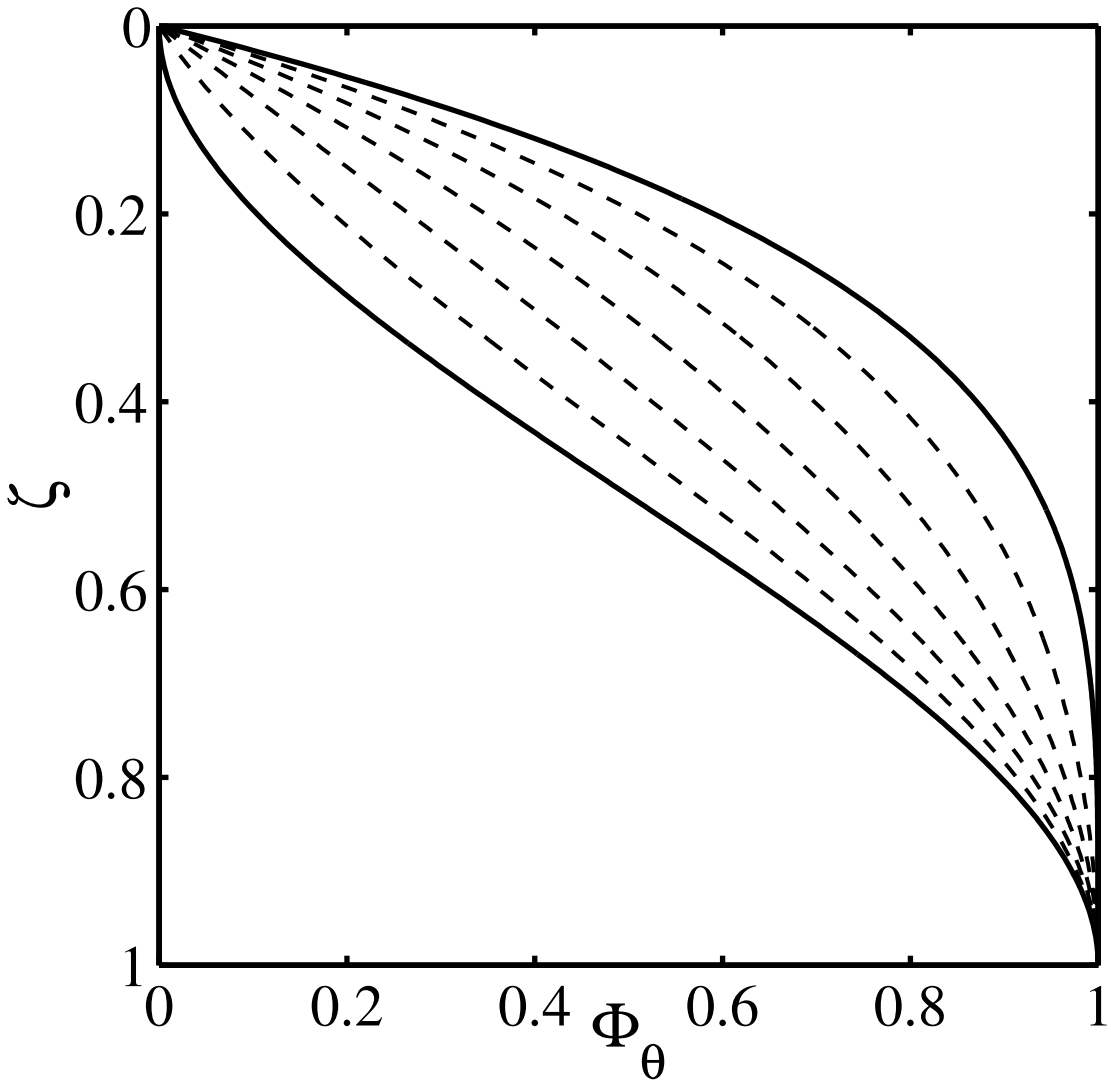

Figure 4. The fourth-order polynomial approximation of the shape function $\Phi_\theta(\zeta)$ with respect to the temperature profile in the thermocline. The curves are computed from Eq. (55) with seven different values of the shape factor C_θ ranging from $C_\theta = C_\theta^{min} = 0.5$, lower solid curve, to $C_\theta = C_\theta^{max} = 0.8$, upper solid curve.

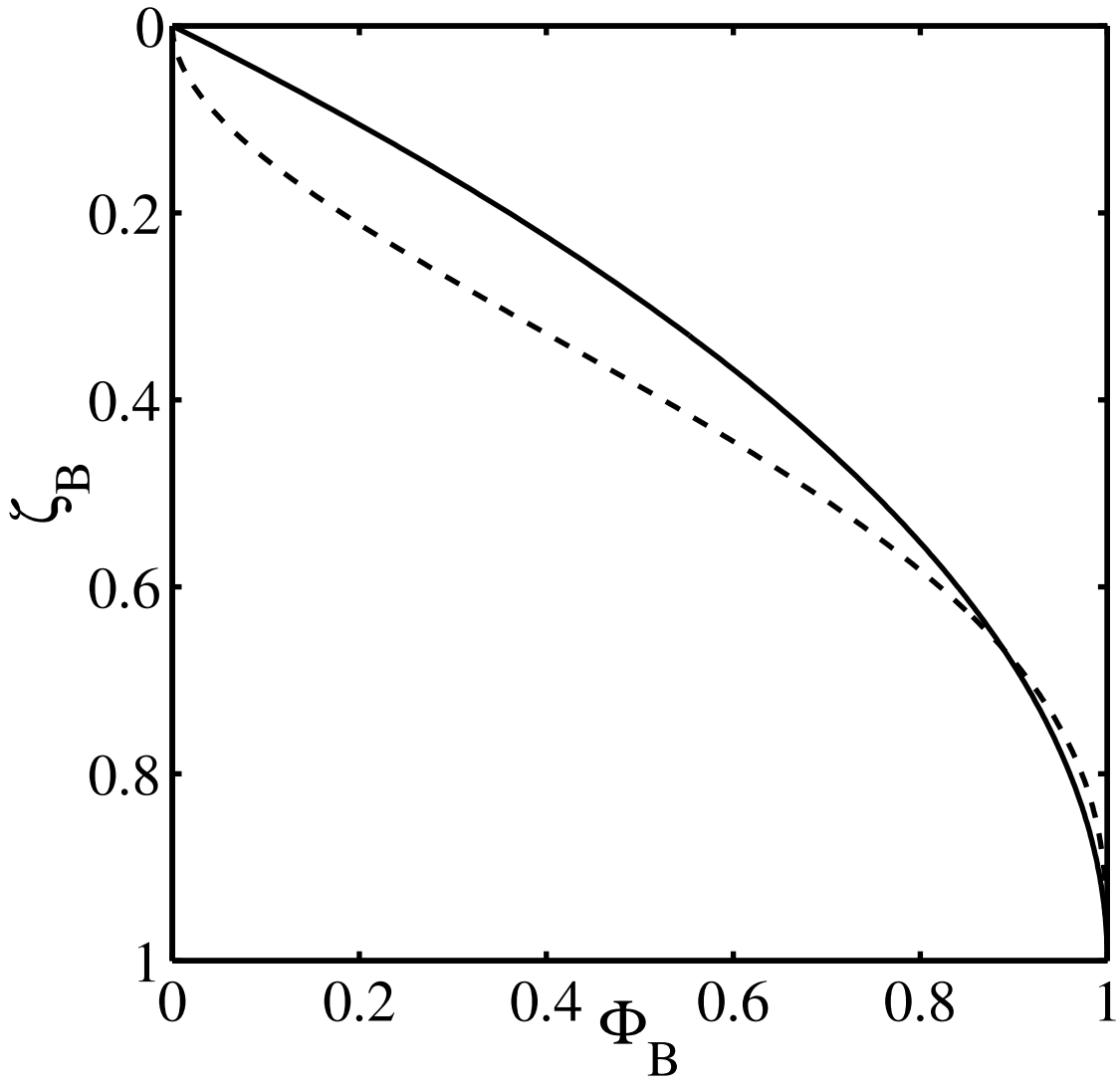

Figure 5. The polynomial approximations of the shape functions $\Phi_{B1}(\zeta_{B1})$, solid curve, and $\Phi_{B2}(\zeta_{B2})$, dashed curve, with respect to the temperature profile in bottom sediments. The curves are computed from Eq. (59).

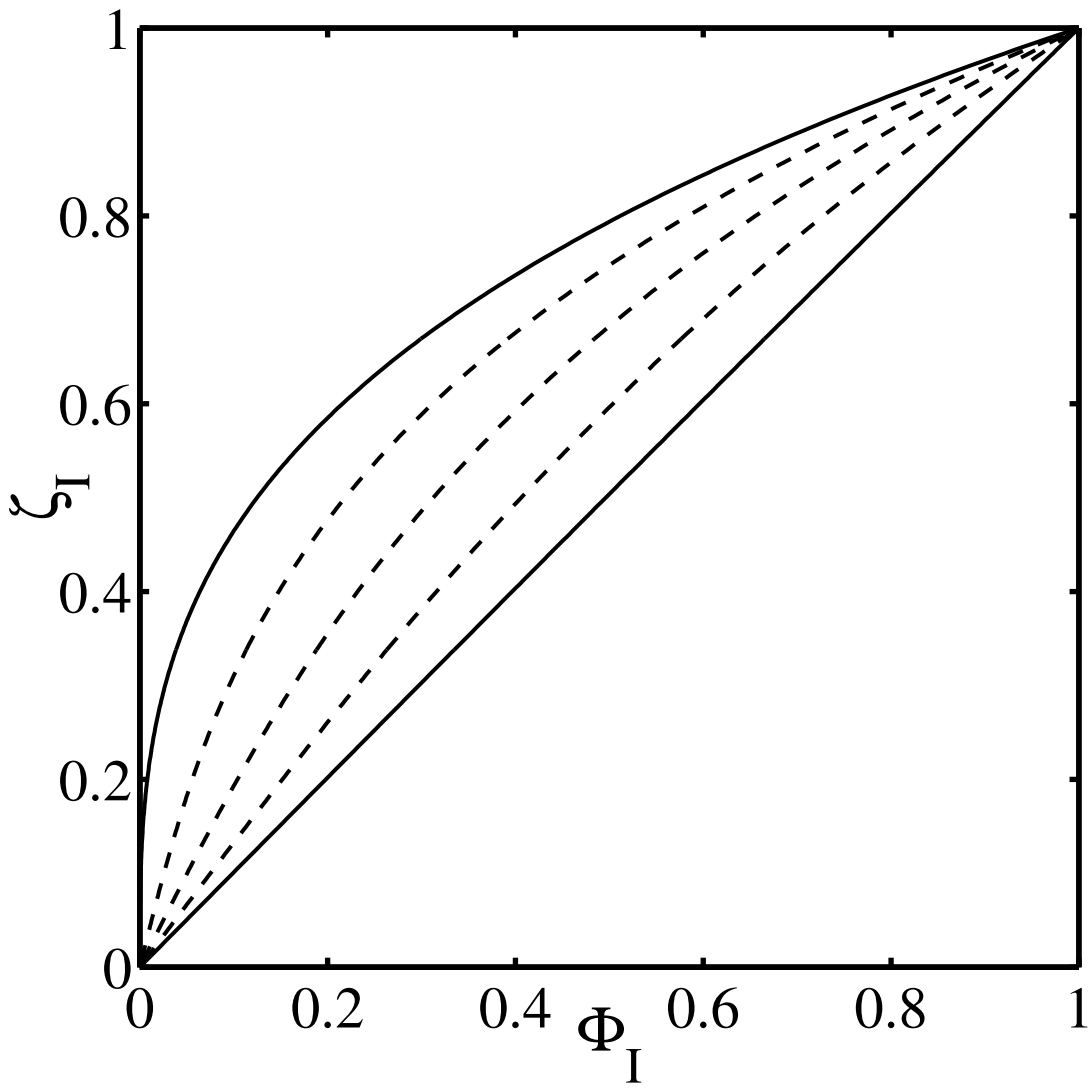

Figure 6. The approximation of the temperature profile shape function $\Phi_I(\zeta_I)$ given by Eq. (60). The curves are computed with $\Phi_{*I} = 2$ and (from right to left) $H_I/H_I^{max} = 0.01$, $H_I/H_I^{max} = 0.25$, $H_I/H_I^{max} = 0.5$, $H_I/H_I^{max} = 0.75$ and $H_I/H_I^{max} = 1.0$.

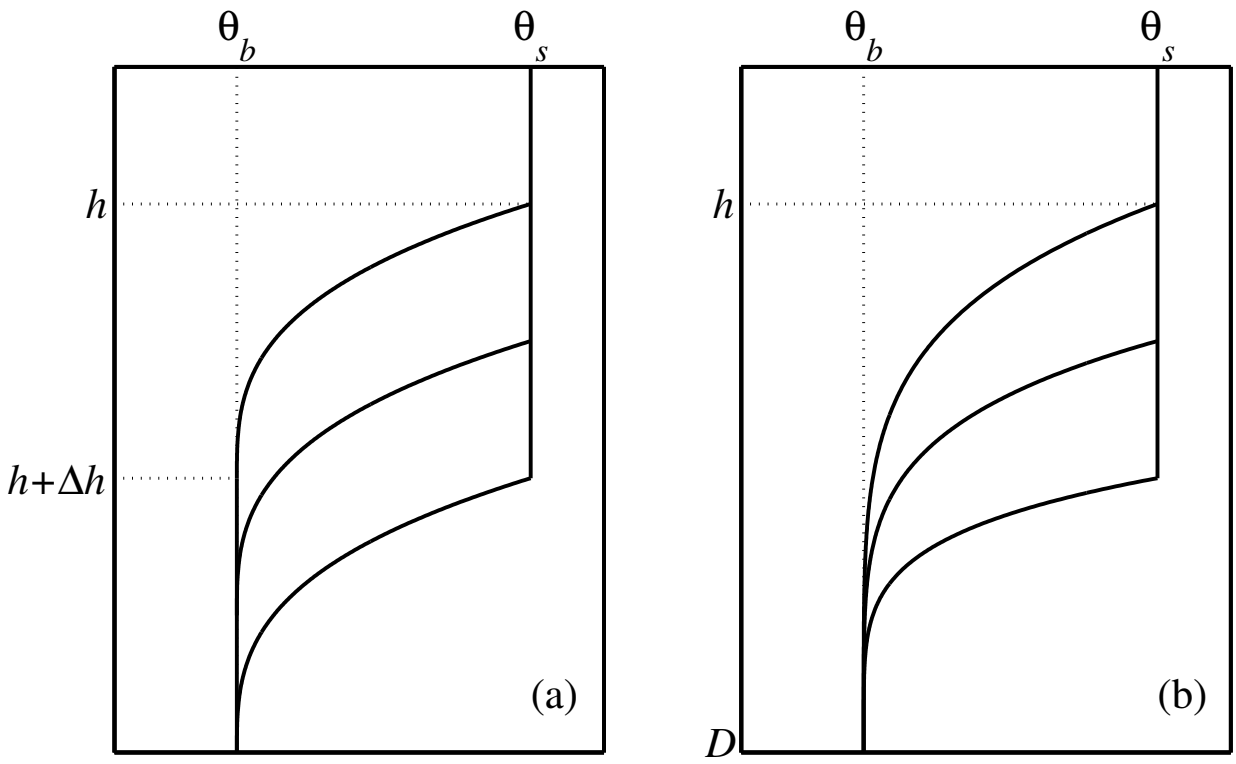

Figure 7. Self-similar temperature profile during the mixed-layer deepening. (a) In a neutrally stratified deep ocean, the mixed-layer depth increases, $dh/dt > 0$, whereas the depth of the thermocline remains constant, $d\Delta h/dt = 0$. (b) In lakes, the thermocline is pressed against the bottom, $\Delta h = D - h$, so that $dh/dt = -d\Delta h/dt$.

Figure Captions

Figure 1. Schematic representation of the temperature profile in the upper mixed layer and in the thermocline. See text for notation.

Figure 2. Schematic representation of the temperature profile in bottom sediments during periods of (a) heating and (b) cooling. Dashed curves show the initial temperature profiles, i.e. the profiles developed towards the end of the previous period of cooling (heating). See text for details.

Figure 3. (a) Schematic representation of the temperature profile in the mixed layer, in the thermocline and in the thermally active layer of bottom sediments. The evolving temperature profile is specified by five time-dependent quantities, namely, the mixed-layer temperature $\theta_s(t)$ and its depth $h(t)$, the temperature $\theta_b(t)$ at the water-bottom sediment interface, the temperature $\theta_H(t)$ at the bottom of the upper layer of bottom sediments penetrated by the thermal wave, and the depth $H(t)$ of this layer. The temperature θ_L at the outer edge $z = L$ of the thermally active layer of the sediments is constant. (b) In case the lake is covered by ice and snow, four additional quantities are computed, namely, the temperatures $\theta_S(t)$ at the air-snow interfaces, the temperatures $\theta_I(t)$ at the snow-ice interfaces, the snow depth $H_S(t)$ and the ice depth $H_I(t)$.

Figure 4. The fourth-order polynomial approximation of the shape function $\Phi_\theta(\zeta)$ with respect to the temperature profile in the thermocline. The curves are computed from Eq. (55) with seven different values of the shape factor C_θ ranging from $C_\theta = C_\theta^{min} = 0.5$, lower solid curve, to $C_\theta = C_\theta^{max} = 0.8$, upper solid curve.

Figure 5. The polynomial approximations of the shape functions $\Phi_{B1}(\zeta_{B1})$, solid curve, and $\Phi_{B2}(\zeta_{B2})$, dashed curve, with respect to the temperature profile in bottom sediments. The curves are computed from Eq. (59).

Figure 6. The approximation of the temperature profile shape function $\Phi_I(\zeta_I)$ given by Eq. (60). The curves are computed with $\Phi_{*I} = 2$ and (from right to left) $H_I/H_I^{max} = 0.01$, $H_I/H_I^{max} = 0.25$, $H_I/H_I^{max} = 0.5$, $H_I/H_I^{max} = 0.75$ and $H_I/H_I^{max} = 1.0$.

Figure 7. Self-similar temperature profile during the mixed-layer deepening. (a) In a neutrally stratified deep ocean, the mixed-layer depth increases, $dh/dt > 0$, whereas the depth of the thermocline remains constant, $d\Delta h/dt = 0$. (b) In lakes, the thermocline is pressed against the bottom, $\Delta h = D - h$, so that $dh/dt = -d\Delta h/dt$.